9950-662

BOEING
ENGINEERING &
CONSTRUCTION
THE BOEING ENERGY
AND ENVIRONMENT DIVISION

Final Report

Air Brayton Solar Receiver
Phase 1

JPL Contract No. 955119

January 5, 1979

AIR BRAYTON SOLAR RECEIVER

Phase I

FINAL REPORT

Prepared By

BOEING ENGINEERING AND CONSTRUCTION

A Division of The Boeing Company
Seattle, Washington 98124

Program Manager
D. K. Zimmerman

Prepared For

Jet Propulsion Laboratory
4800 Oak Grove Drive
Pasadena, California 91103

JPL Contract No. 955119

Table of Contents

1.0 Introduction

1.1 INTRODUCTION

This report describes the results of a six month analysis and conceptual design study of an open cycle "Air Brayton Solar Receiver" (ABSR) for use on a tracking, parabolic solar concentrator. The ABSR, which includes a buffer storage system, is designed to provide inlet air to a power conversion unit (PCU). This report describes the results of Tasks 1 through 4; parametric analyses, conceptual design, interface requirements, and production cost estimates. Task 5, the Phase II proposal, is contained in a separate document.

BEC has drawn extensively on the experience and technology developments of recent design and test programs of a similar nature. Hence, the selected concept is not only current in its state-of-the-art, but all the selected materials have been previously tested and proven in similar environments.

This study has led to the selection of a conceptual design that utilizes low cost commercially available materials and fabrication methods. The design features have been optimized to yield a zero maintenance, low cost, high efficiency concept that will provide a 30 year operational life. The design is fully responsive to the requirements of the Statement of Work, with no exceptions.

1.2 STUDY APPROACH

The ABSR program was conducted in four major parts: parametric analyses; design evaluation; conceptual design development; and development of production cost data.

The parametric analysis began with a review of the ABSR requirements. These requirements formed the basis for the performance analysis which determined receiver and storage system size as a function of the specified design parameters. The parametric analysis also investigated various methods of system controls.

The design evaluation process utilized specific design point information to allow selection of the ABSR concept most suited to give high performance with low pressure drop, cost and weight.

The conceptual design development overlapped both the design evaluation and the production cost development since predicted costs were important factors in the evaluation process. When the lowest cost design concept was finally identified, design and assembly details were refined and finalized.

The final part of the study was to generate projected cost data for production runs between 100 and 1,000,000 units per year.

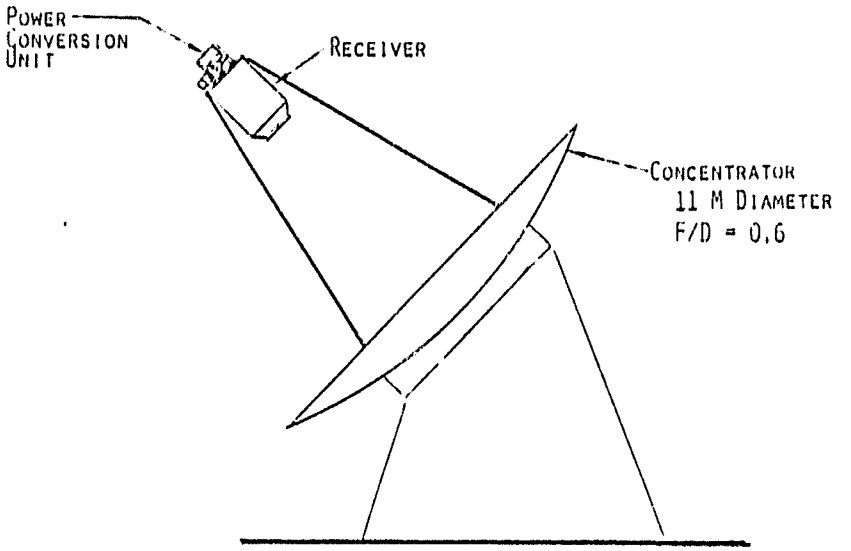

1.3 SUMMARY

1.3.1 Relative Size

The artist's concept shows the BEC receiver mounted atop an 11 meter diameter parabolic concentrator. In terms of relative size, the high efficiency receiver shades approximately 1.4% of the concentrator area.

The sketch shows the support struts from the concentrator terminating at a mounting ring flange at the upper end of the receiver. This enables either the receiver or the PCU to be independently removed from the support structure. As discussed later, the receiver structure could support the PCU. This would give the option of moving the mounting ring closer to the aperture enabling the struts to be in line with the center-of-gravity of the combined load.

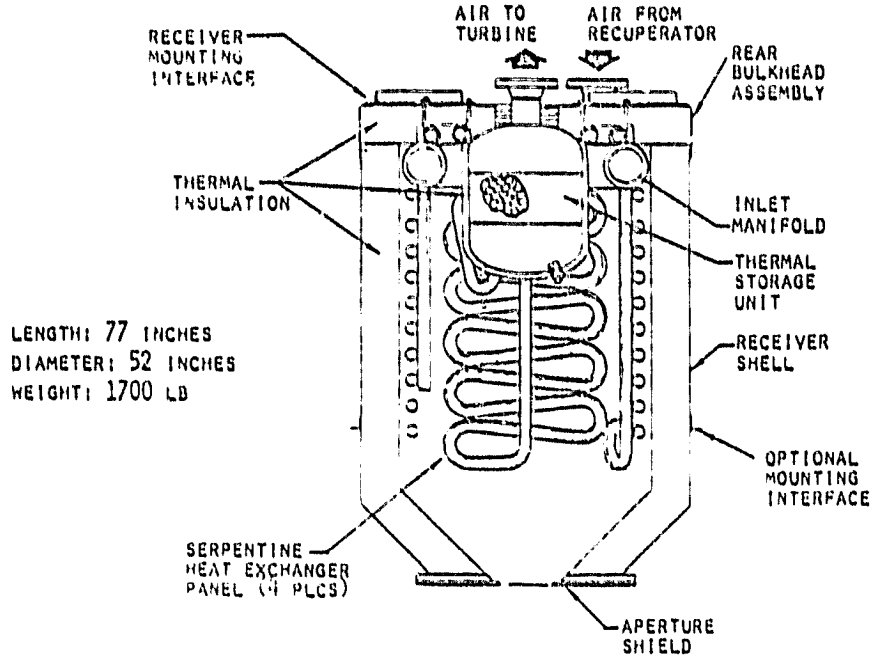

1.3.2 Sectional View of Selected Concept

The above sketch represents a sectional view of the ABSR. Major features are:

- The receiver/PCU physical interface is made extremely clean by locating the storage tank inside the receiver. The single inlet and single outlet air connections between the receiver and PCU are through four or five inch bolted flanges. All internal air path connections are welded.
- The air flow path is from the recuperator through a short pipe to the circular inlet manifold, where it is evenly distributed to four serpentine shaped heat exchangers operating in parallel; the heat exchangers discharge the heated air into the bottom end of the storage tank; all air continuously passes upwards through the storage pebble bed and out through a short pipe to the PCU turbine. This flow path places the coldest (inlet) air in the region of the highest direct solar heat flux enabling the heat exchanger tubes to approach a uniform temperature condition.

- o The cylindrical receiver shell and the rear bulkhead assembly are insulated with six inches of rigid, vacuum-formed insulation. The shell and its insulation can be removed from the rear bulkhead without disturbing the rest of the receiver or the PCU.
- o The aperture shield is a composite of zirconia board, alumina board, and Inconel 601 superalloy sheet. It is bolted to the receiver shell allowing easy replacement in case of damage.

- o The ABSR has no moving parts and materials and allowables are selected for 30 year life; this eliminates the need for any planned maintenance.

1.3.3 Design Features

The ABSR design concept incorporates the following features:

- o Clean Interfaces
  - . The top of the receiver is clean to allow easy mounting of the PCU.
  - . There are no flow controls which could provide a variable flow resistance to the PCU.
  - . The ABSR is compatible with either mode of PCU operation: constant speed or constant inlet temperature.
  - . Field alignment of the aperture can be accommodated by shimming at the receiver flange.
  - . Response capability is adequate to accommodate sun acquisition at mid-day.

- o Proven Materials
  - . Commercially available metal alloys, insulation, and aperture shield materials are used which have been tested and proven by BEC in similar applications.
  - . The selected storage media is commercially available and has been industry proven for application in this temperature range.

- State-of-the-Art Design
  - ASME and ANSI codes are followed wherever possible. Allowables for the heat exchanger material are not code approved but the ASME code approach was used to obtain design allowables.
  - Design features and processes have been demonstrated in previous BEC development programs.

- Simple Operation
  - The ABSR will be instrumented with four thermocouples that sense heat exchanger tubing temperature. In the event of low air flow from the PCU or greater than design-value insolation, the receiver is fully protected by bypassing part of the compressor outlet air around the recuperator.
  - Other than the thermocouples just mentioned, the ABSR has no controls, sensors, or logic requiring interfaces with the PCU or its control system.

- Minimal Maintenance
  - The ABSR is designed for 30 year life with no scheduled maintenance or replacement.
  - There are no moving parts.
  - All materials including the internal insulation are weather resistant. The presence of moisture, dust, sand, ice or snow will not cause any damage or long term degradation in performance.

- Proven Test Approach
  - The receiver test program utilizing an external air source combined first with a solar simulator and later with an operational solar collector are concepts based on a current BEC test program for the Electric Power Research Institute (EPRI).

- Mass Producible/Low production Costs
  - The selected design minimizes the number of tube welds.
  - Serpentine heat exchanger shape can be formed by bending on existing industry machines.
  - An assembly line production technique is planned, which will rely on outside suppliers and specialty fabricators for production of nearly all components.

- Design Point Operation
  - When supplied with 0.533 lbs. per second air at 1050°F and 35 psia, the ABSR will supply air at 1500°F. The overall pressure drop is 3.5% at this condition. The 68.5 kW thermal output requires 74.6 kW input to the receiver (91.8% efficiency, neglecting convection losses). Convection losses are calculated to be less than 8 kW, so 85 kW from the concentrator is more than adequate for the ABSR to meet performance requirements.
  - It should be noted that the ABSR is capable of supplying air at temperatures somewhat in excess of 1500°F since the design concept for receiver protection is to measure and limit heat exchanger temperatures. If this is not acceptable for the PCU, an air temperature sensor which also commands recuperator bypass can readily be installed.

2.0 Requirements

2.1 GENERAL REQUIREMENTS

The Air Brayton Solar Receiver and storage systems concepts evaluated and selected by BEC during this study contract were in compliance with the general requirements set forth in the Statement of Work:

- "The ABSR design is to be representative of Industries best current state-of-the-art practice..."
- "...low cost design and fabrication for equipment of this type."

2.2 DESIGN POINT - PERFORMANCE REQUIREMENTS

The Task 1 parametric analyses utilized the following matrix of design point definitions supplied by JPL as Exhibit I of the Statement of Work.

Peak Thermal Input Power	50, 90, 150 KW_{th}
Fluid Outlet Temperature	1000, 1300, 1500, 1600 ^{o}F
Fluid Inlet Temperature	900, 1000, 1100, 1200 ^{o}F
Fluid Flow Rates	0.004, 0.008, 0.012, 0.016 #/sec/KW_{t}
Fluid Inlet Pressures	30, 45, 60, 75 psig
Fluid Pressure Loss	5 percent maximum
Buffer Storage Capacity	10 minutes

The Task 2 conceptual design phase of the program utilized specific design point data supplied by JPL at the conclusion of Task 1.

Peak Thermal Input Power	85 KW_{t}
Fluid Outlet Temperature	1500 ^{o}F
Fluid Inlet Temperature	1050 ^{o}F
Fluid Flow Rate	0.533 lbs/sec
Fluid Inlet Pressure	35 psia (20.3 psig)
Fluid Pressure Loss	5% causes serious degradation in system performance. 2% would be excellent
Buffer Storage Capacity	10 minutes

2.3 DESIGN REQUIREMENTS

The general requirements for the design and construction of the ABSR are:

- o 30 year design goal lifetime
- o minimum size and weight
- o insensitive to orientation with respect to gravity

Specific requirements are:

- o Normal Operation
  - a) 30 mph steady state winds with 20% gust factor
  - b) California high desert gust spectrum
  - c) temperatures, $0^{o}F$ to $125^{o}F$
  - d) humidity 0 - 100%
  - e) dust - blowing California desert dust and sand
  - f) altitude - 0 to 6000 feet

- o Survival (no damage or permanent set)
  - a) winds to 100 mph (any direction)
  - b) seismic lateral accelerations of 0.25g in any direction combined with 1g gravity loading.
  - c) snow and glazed ice (1 inch thick) combined with 1g gravity loading.

- o Codes and Standards
  - a) ASME Boiler and Pressure Vessel Code, Section VIII, Pressure Vessels, Div. 1, latest revision.
  - b) California Occupational Safety and Health Administration; Safety Requlations.

3.0 System Evaluation

3.1 Receiver

Receiver thermal analyses were conducted in two phases: parametric analysis and detailed analysis. The parametric analysis utilized several simplifying assumptions and a limited thermal model to scope the importance of design variables. The detailed analysis employed a large but generalized finite difference representation of the receiver system. Both phases of the analyses are described in the following paragraphs.

3.1.1 Parametric Analysis

3.1.1.1 Receiver Parameters

The parameters involved in evaluation of the receiver may be categorized as operation, configuration and performance parameters.

- Operation Parameters
  - Peak Thermal Power Input
  - Fluid Outlet Temperature
  - Fluid Inlet Temperature
  - Fluid Flow Rate
  - Fluid Inlet Pressure

- Configuration Parameters
  - Receiver Aperture: Location, Size
  - Receiver Cavity Geometry
  - Receiver Wall: Material Thickness
  - Heat Exchanger:Material, Geometry, Location

- Performance Parameters
  - Pressure Drop
  - Efficiency
  - Component Temperatures

The final evaluation of a given receiver design would be based on its integration into an overall system optimization scheme. Since such a scheme would be unwieldy at the concept evaluation stage, design goals and guidelines were established for the receiver evaluation. Those pertinent to the receiver parametric analysis are:

- 30 Year Lifetime
- Minimum Size and Weight
- Minimum Cost

These design goals and guidelines were used, along with previous BEC experience in receiver design and fabrication, to narrow the scope of the parametric analysis. In particular, the following parameters were fixed in the early stages of the analysis:

- Circular Aperture Located at Focal Plane
- Heat Exchanger Tubes of Inconel Alloy 617
- Cylindrical Receiver Shape
- Kaowool Insulation Material
- Structural Steel used on Receiver Exterior

These choices were open to re-evaluation during the analysis if they produced any undue penalties in receiver performance.

3.1.1.2 Receiver Cavity and Wall

The receiver cavity and wall analysis can be conveniently separated from the heat exchanger analysis by assuming various heat exchanger tube temperatures in the cavity analysis. The parametric cavity analysis was based on a four node model of a cylindrical cavity with length equal to diameter. These nodes represented the aperture, top, bottom, and sidewall. The sidewall was assumed to be covered by axial heat exchanger tubes with a spacing-to-diameter ratio (s/d) of 2.5. The direct solar flux was assumed to be uniformly distributed over the top and sidewall of the cavity. The cavity wall temperatures and aperture radiation (reflected solar and IR) were determined for various cavity sizes. The model used an eight (8) inch diameter aperture. This aperture size was based on maximizing the net energy capture for a 1700^{o}F cavity and early flux mapping data.

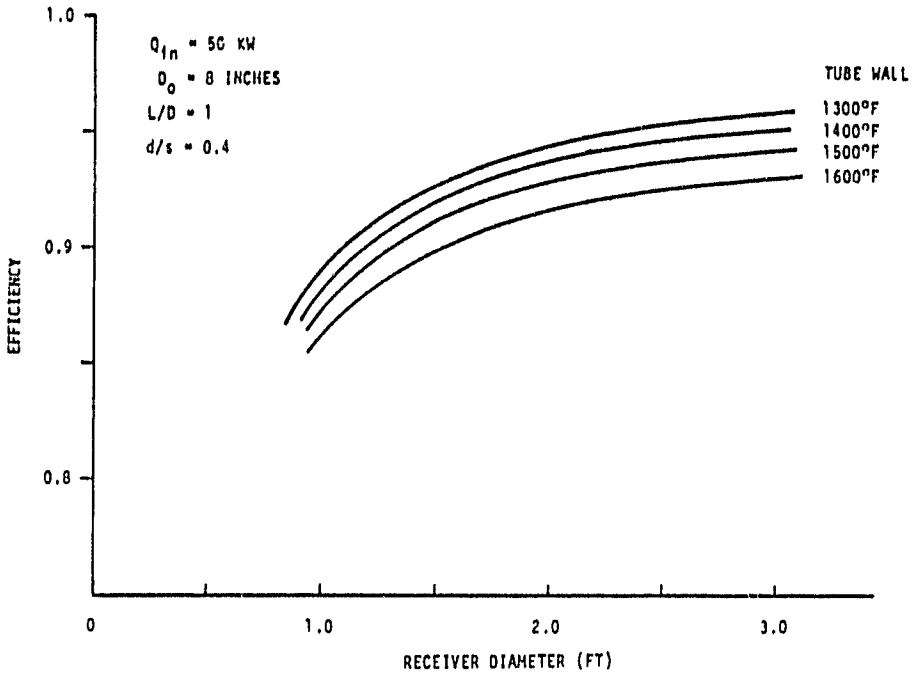

The radiant efficiency of the cavity as a function of cavity size at various tube temperatures is shown in the above figure. These results show that it should be relatively easy to achieve a radiant efficiency greater than 90%. Cavities with length-to-diameter ratios greater than one give higher efficiencies. The other major result of this simple analysis is that the insulation temperature will remain below 2000^{o}F (the upper limit of Kaowool insulation) for cavity diameters greater than about two feet.

The minimum insulation wall thickness required to keep the structural steel on the cavity exterior below 500^{o}F was determined by assuming the interior temperature to be at 2000^{o}F and the external convective heat transfer coefficient to be 1 BTU/ft^{2}-hr-^{o}F. The minimum insulation thickness was found to be about two inches. This analysis showed the basic receiver concept to be feasible with no undue penalties resulting from using Kaowool insulation.

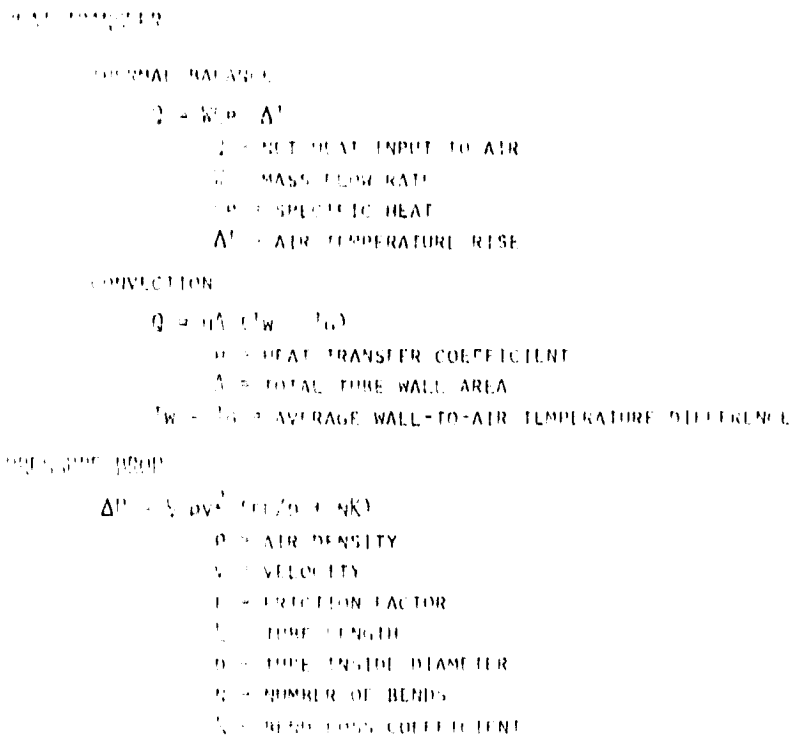

3.1.1.3 Heat Exchanger

The heat exchanger parametric analysis can be separated from the receiver cavity performance by specifying the net heat input to the gas instead of the thermal input to the cavity. The basic relationships for the heat exchanger analysis are shown at the top of the page. By using the fully developed turbulent flow equations for heat transfer coefficient and friction factor, these basic relationships can be used to write parametric equations for tube length and tube diameter as shown on the following page.

BASIC ASSUMPTIONS

HEAT TRANSFER COEFFICIENT

$$H = 0.021\, K/D\ Re^{0.8}\ Pr^{1/3}$$

K = THERMAL CONDUCTIVITY
Re = REYNOLDS NUMBER
Pr = PRANDTL NUMBER

FRICTION FACTOR

$$F = 0.316/Re^{0.25}$$

AIR PROPERTIES TAKEN AT 1250°F

TUBE LENGTH

$$L = \frac{0.8253(Q/N)^{0.5949}\ \Delta T^{0.6076}}{\alpha^{1.2025}\ p^{0.7050}\ (T_W - T_G)^{1.2025}} \quad (FT)$$

TUBE INSIDE DIAMETER

$$D = \frac{0.01806(Q/N)^{0.4937}}{\alpha^{0.253}\ p^{0.5063}\ (T_W - T_G)^{0.253}\ \Delta T^{0.2405}} \quad (FT)$$

N = NUMBER OF TUBES

α = PERCENT PRESSURE DROP

P = AIR PRESSURE (ATM)

Q = HEAT INPUT TO AIR (BTU/HR)

T = TEMPERATURE (°F)

The number of tube bends is dependent on the specific heat exchanger configuration and inclusion of their effects at this point would unduly complicate the analysis.

The total heat exchanger surface area (A) required per unit heat input is given by:

$$(A/Q) = \frac{0.0469(Q/N)^{.089}\ \Delta T^{.367}}{\alpha^{.455}\ p^{.911}\ (T_w - T_g)^{1.455}} \quad Ft^2/(BTU/hr)$$

The net heat input to air Q, gas temperatures T_g and ΔT, allowable pressure drop α, and pressure P are determined primarily by the gas turbine performance characteristics. The number of heat exchanger tubes N and allowable tube wall temperature Tw are determined by the heat exchanger design. The heat exchanger envelope size (cavity surface area Ac covered by heat exchanger) is given by:

$$(A_c/Q) = (A/Q)\cdot(s/d)/\pi$$

where s/d is the tube spacing-to-diameter ratio.

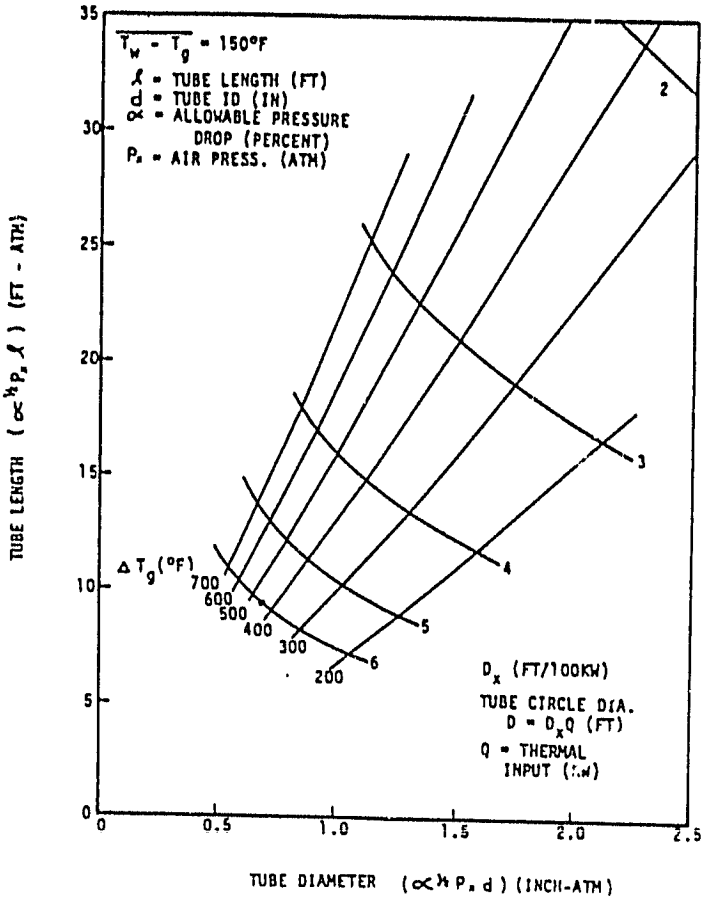

In addition to the envelope size, the shape of the heat exchanger envelope is also important. For example, a heat exchanger utilizing a large number of tubes will reduce the envelope size, however, this will require a cavity with a small length-to-diameter ratio. This cavity shape would produce large solar blockage of the collector and would have greater reflection losses than cavities with larger length-to-diameter ratios. The figure at the top of the page shows heat exchanger sizing, for straight tubes, with the heat exchanger envelope diameter as an independent variable. This particular figure pertains to an average wall-to-gas temperature difference of 150°F and a tube spacing-to-diameter ratio of 2.75. Similar figures can be generated for other temperature differences and spacing-to-diameter ratios. As a sizing example, consider the case of 50 KW input to the air, 4% allowable pressure drop, 4 atmospheres pressure and a gas temperature rise of 500°F. For this case a 2 ft. diameter heat exchanger envelope would require 200 tubes each 2 ft. long with a 0.1375 inch diameter. Detailed heat exchanger sizing requires a design point definition to further narrow the scope of the parametric analysis.

[illegible] POINT DATA

W = [illegible] LB/SEC

ΔT = [illegible]

Q = W·Cp·ΔT = 2.34×10^5 BTU/HR (68.5 KW)

P = [illegible] ATM

[illegible] LENGTH

$$L = \frac{37230}{\alpha^{0.2025} N^{0.5959} (T_W - T_G)^{1.2025}} \quad \text{(FT)}$$

[illegible] INSIDE DIAMETER

$$D = \frac{1.109}{\alpha^{0.253} N^{0.4937} (T_W - T_G)^{0.253}} \quad \text{(FT)}$$

STRAIGHT TUBES — RELATIONSHIPS MORE COMPLEX FOR TUBES WITH BENDS

3.1.2 Configuration Evaluation

3.1.2.1 Design Point Data and Tube Sizing

The pertinent design point data and the resulting parametric tube sizing equations are given at the top of the page. The air temperature rise of 450°F is based on 1050°F air inlet and 1500°F air outlet design point temperatures. The remaining parameters involved in sizing the heat exchanger tubes are allowable pressure drop, number of tubes and average wall to gas temperature difference. The allowable pressure drop was not explicitly given in the design point data; however, it was stated that a 5 percent pressure drop would result in serious performance degradation while a value of 2 percent would be excellent. The number of heat exchanger tubes is dependent on the heat exchanger configuration. The maximum allowable tube wall to gas temperature difference is limited by the decrease in allowable stress with increasing temperature.

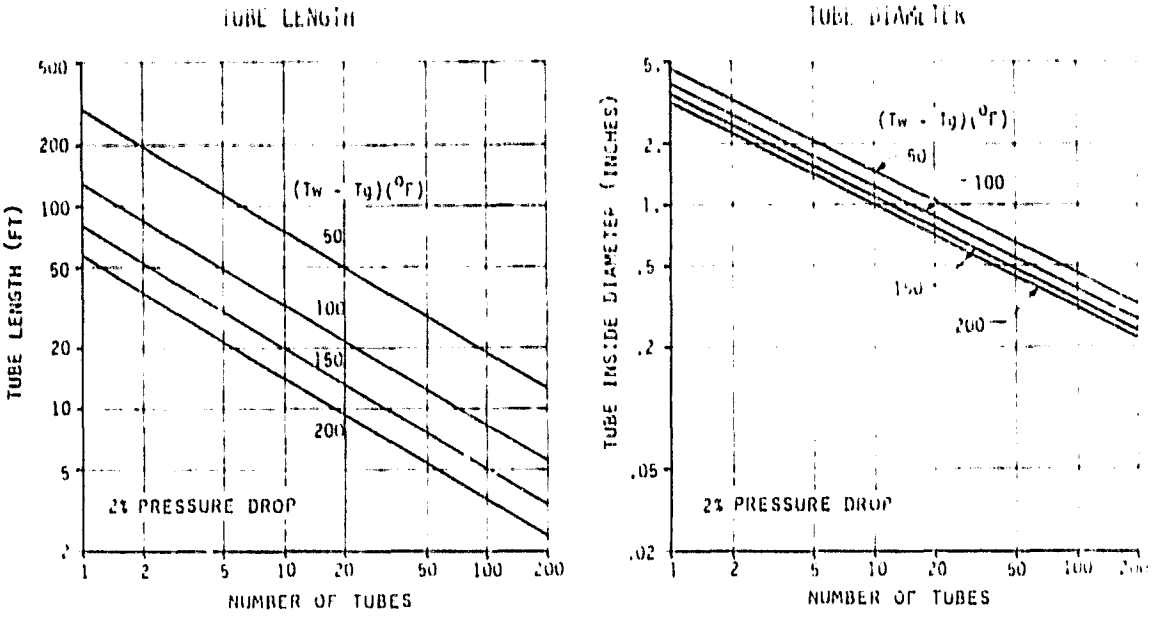

Heat exchanger tube length and inside diameter are shown as a function of the number of tubes in the above figure. Curves are given for various wall-to-gas temperature differences for the 2 percent pressure drop case. Similar curves can be drawn for other pressure drop conditions. The sensitivity of tube length and diameter to changes in allowable tube wall temperature and pressure drop are shown in the figures below. The curves are normalized to a wall-to-gas temperature difference of 150°F and a pressure drop of 2 percent, respectively. As can be seen from the figures, the allowable tube-to-gas temperature difference has a much greater impact on tube size than does the allowable pressure drop.

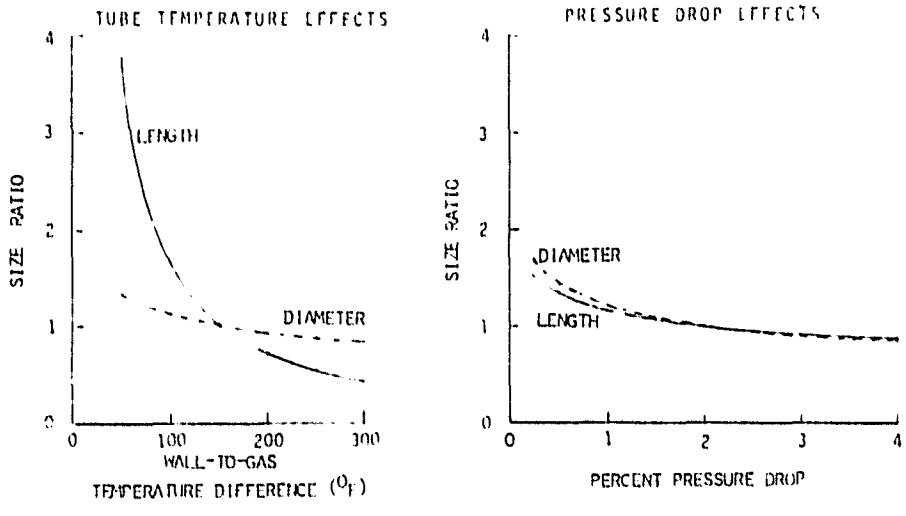

MINIMUM EFFECT ON REST OF SYSTEM

- SIZE
- WEIGHT
- PRESSURE DROP

MINIMIZE COST

- SINGLE CONTROL VALVE - REQUIRES PARALLEL FLOW PATHS TO BE EXPOSED TO IDENTICAL HEAT FLUXES.
- MINIMUM NUMBER OF COMPONENTS
- SIMPLE CONFIGURATION

MINIMIZE STRESS PROBLEMS

- AIR FLOW PATH FROM HIGH FLUX TO LOW FLUX REGION TO MINIMIZE TUBE WALL TEMPERATURE.
- ALLOW AS MUCH FREEDOM OF MOVEMENT AS POSSIBLE TO MINIMIZE THERMAL STRESSES.

3.1.2.2 Heat Exchanger Configuration

The general considerations involved in selecting a heat exchanger configuration are given above. Preliminary screening eliminated several configuration concepts which utilized parallel air flow paths not exposed to identical heat flux environments. These concepts would require individual flow control valves to maintain a 1500^{o}F air outlet temperature. Helical tube configurations were also eliminated because they lack freedom of movement to accommodate differential thermal expansion effects.

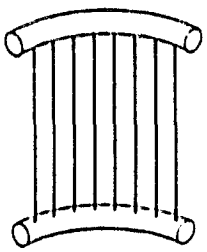

STRAIGHT TUBES

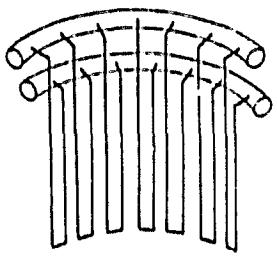

BMSR-TYPE

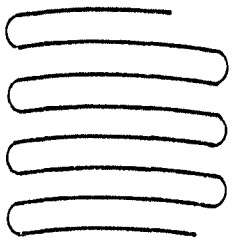

SERPENTINE

ADVANTAGES		
SIMPLE CONFIGURATION	PRIOR EXPERIENCE	FEW TUBES
IDEAL FLOW PATH	FREEDOM OF MOVEMENT	FREEDOM OF MOVEMENT
	MANIFOLDS AT SAME END OF RECEIVER	GOOD FLOW PATH

Three candidate heat exchanger configuration wre selected for more detailed evaluations. These are straight tube, bent (BMSR-type) tube and serpentine tube configuration. The artists concepts shown above are a schematic representation of these configurations. The straight tube concept is the simpliest configuration and has an ideal flow path for the case of direct solar flux impinging on the tubes since the lower temperature inlet air can be introduced at the peak flux location. Straight tubes, however, lack an inherent freedom of movement which requires additional design complexity including the use of bellows to reduce thermal stresses.

Bent tubes have been successfully used in the BMSR and have an inherent freedom of movement which minimizes thermal stress problems. However, for the present application in which the tubes are exposed to direct solar flux, the air flow path does not help in reducing the tube wall temperature at the peak flux location.

Serpentine tubes provide a near ideal air flow path and have an inherent freedom of movement. This configuration has the additional advantage of utilizing a small number of tubes which reduces the fabrication cost.

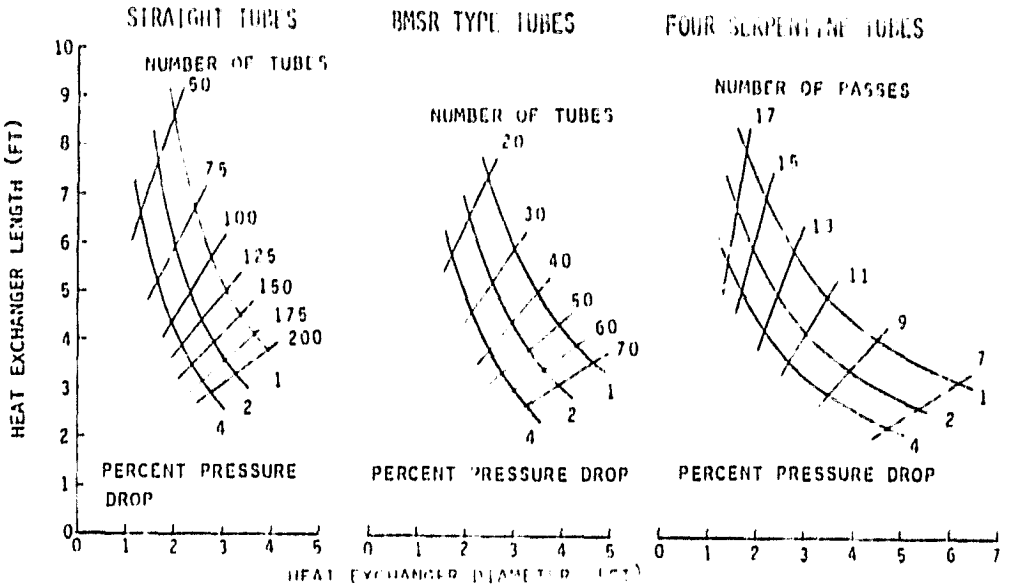

Preliminary sizing of the heat exchanger envelope for the candidate configurations is shown above. This sizing is based on a tube wall-to-gas temperature difference of 150°F and a tube spacing-to-diameter ratio of 2.5. The sizing for the four tube serpentine configuration takes into account the effect of the tube bends on heat transfer and pressure drop. The curves show the straight tube configuration to be slightly smaller than the other configurations. This difference in size is relatively unimportant in the configuration evaluation.

The effect of allowable pressure drop on heat exchanger size is shown graphically below. A design pressure drop of 2 percent was chosen for the heat exchanger. This allows the total system pressure drop to be maintained below 4 percent and provides a reasonable trade between size and pressure drop.

- FOUR SERPENTINE TUBES
- ELEVEN TUBE PASSES
- $T_W - T_G = 150^{\circ}F$
- TUBE SPACING/DIAMETER = 2.5

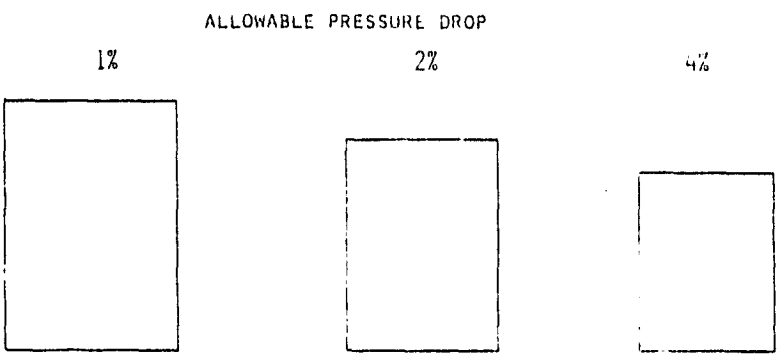

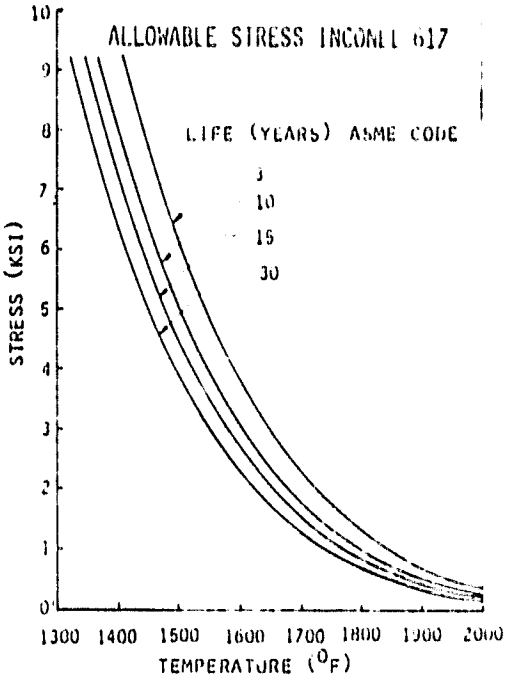

A major factor in evaluation of the candidate configuraitons is the stress in the tube wall. The allowable stress for Inconel 617 is shown above as a function of temperature for various years of design life. The decrease in allowable stress with increasing temperature will limit the maximum tube wall-to-gas temperature difference. This, in turn, will establish the minimize size for the heat exchanger envelope and, consequently, the minimum receiver size.

A maximum tube temperature of 1600°F has been selected for the baseline design. A preliminary stress analysis indicates that the tube working stresses are below the allowables at this temperature.

STRESS	CONFIGURATION		
	STRAIGHT	BMSR	SERPENTINE
PRESSURE	< 1000 PSI	< 1000 PSI	< 1000 PSI
RADIAL TEMPERATURE GRADIENT	NEGLIGIBLE	NEGLIGIBLE	NEGLIGIBLE
LINEAR EXPANSION	*95,000 PSI	** 7,500 PSI	< 1000 PSI
CIRCUMFERENTIAL TEMPERATURE GRADIENT	*9,500	SMALL	SMALL
GRAVITY LOAD	SMALL	SMALL	SMALL

* STRAIGHT TUBES REQUIRE BELLOWS.
** BMSR USES ADDITIONAL TUBE LENGTH AT MANIFOLDS TO REDUCE STRESS.

A preliminary evaluation of the potential stress levels for each candidate configuration is summarized in the table on the following page. The stress level due to the internal air pressure is small for all practical tube diameters and wall thicknesses. The thin tube wall possible with the low air pressure all eliminates any potential stress problem arising from the temperature gradient through the tube wall.

The linear thermal expansion produces unacceptable stress levels in the straight tubes and BMSR-type tubes. Expansion bellows would be required to reduce this stress in the straight tube configuration. The BMSR using additional heat exchanger tube length at the manifolds to reduce this stress. This stress is small in the serpentine tube configuration since the tube wall temperature difference between adjacent tube passes is small. The circumferential temperature gradient around the tube wall will give use to a bending moment in the straight tubes. Bellows at the tube ends would reduce the stress to an acceptable level. Both BMSR type and serpentine configuration allow the tubes to bend and consequently the stress due to the circumferential temperature gradient is minimized. The gravity load should produce no stress problems for any of the configurations.

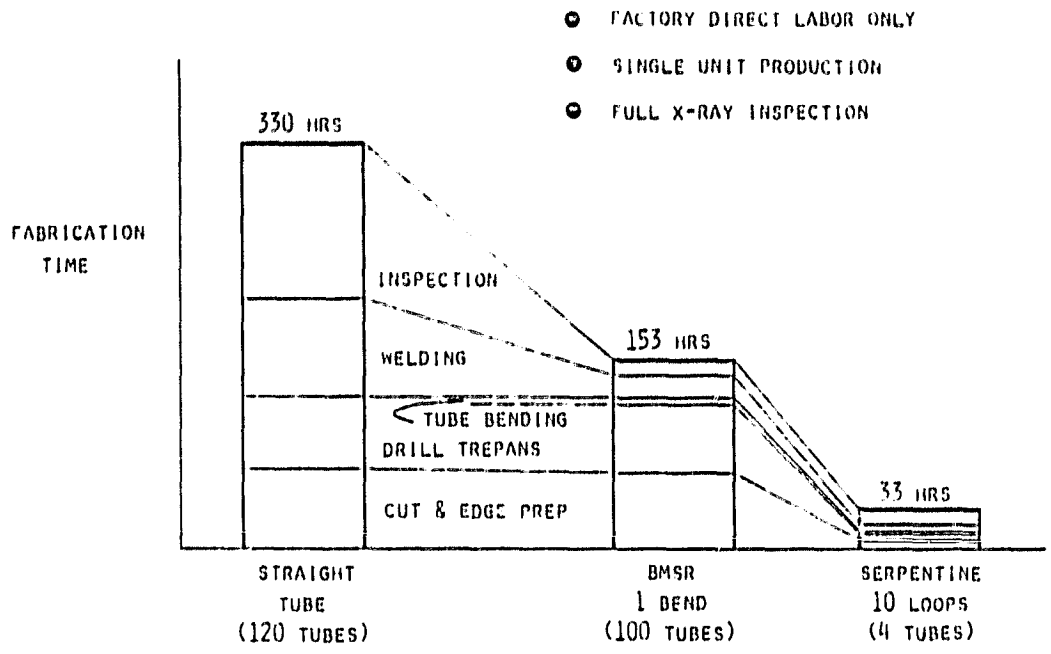

An estimate of the fabrication costs for typical candidate heat exchanger configurations is shown schematically in the above figure. The four tube serpentine configuration has a large fabrication cost advantage over the straight tube and BMSR type tube configurations. Based on cost, stress and flow path considerations, the four tube serpentine configuration was selected as the baseline heat exchanger concept.

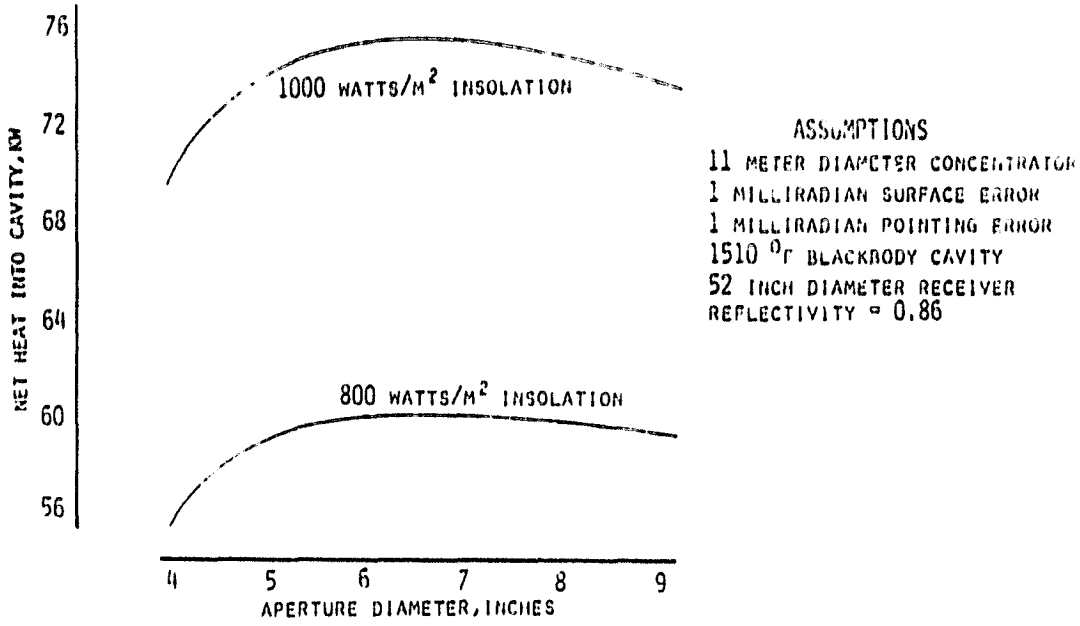

3.1.2.3 Receiver Configuration

The basic receiver configuration consists of aperture size, insulation thickness and receiver shape. The aperture size can be optimized by maximizing the net energy capture by the cavity. The above figure shows the net energy capture as a function of aperture diameter. As the aperture size is increased it admits more of the solar flux, from the collector, into the cavity. Increasing the aperture size also allows more energy to escape from the cavity. The optimum size depends on the focusing properties of the collector and the effective cavity temperature. The above figure shows the optimum aperture diameter to be between 6 and 7 inches for the stated assumptions. A baseline aperture diameter of 8 inches was selected based on earlier collector focusing parameters. In the final receiver design the aperture size can be readily changed to maximize the net energy capture for updated collector performance data.

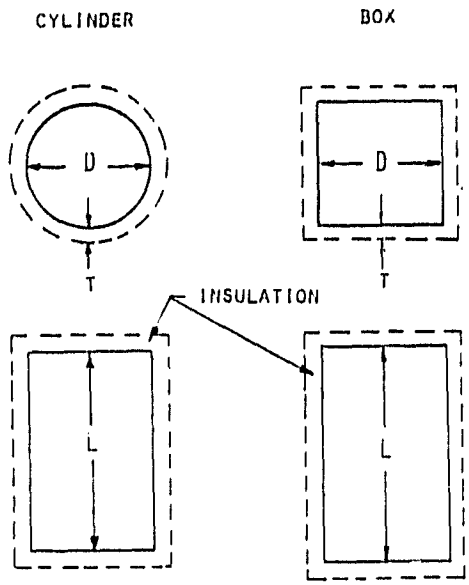

ITEM	CYLINDER	BOX
PRESSURE DROP	2%	2%
PEAK TUBE WALL TEMPERATURE	1600°F	1600°F
SIZE D	3 FT	3 FT
L	5.36 FT.	5.5 FT.
HEAT EXCHANGER TUBE WEIGHT	74 LB	98 LB
BLOCKED AREA		
T = 3.5 INCHES	10.1 FT^2	12.8 FT^2
T = 6.0 INCHES	12.6 FT^2	16.0 FT^2
RECEIVER EFFICIENCY		
T = 3.5 INCHES	85%	82%
= 6.0 INCHES	90%	88%
SHAPE SELECTION	*	

With the selected serpentine heat exchanger configuration it became reasonable to consider a cavity with a square cross-section. This type cavity would eliminate the need of an extra bending operation in fabricating the heat exchangers. The above figure shows a comparison between cylindrical and box shape receivers. This comparison shows the efficiency, size and weight of the box shape receiver to be inferior to the cylindrical receiver.

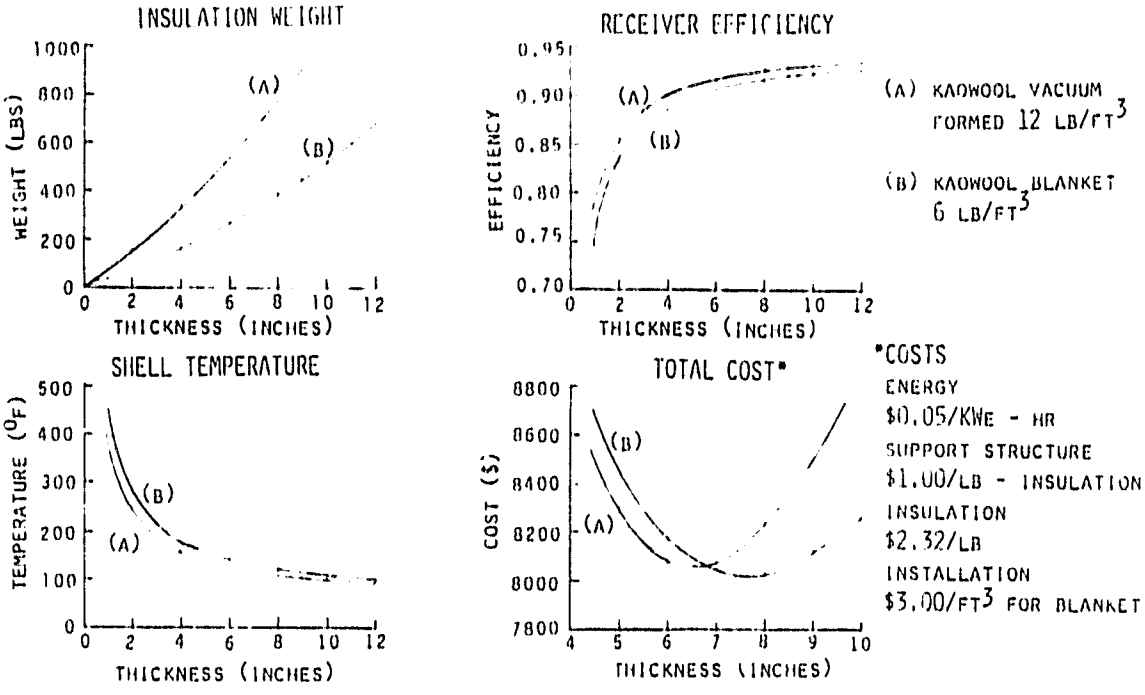

The optimum insulation thickness can be determined by minimizing the total system costs affected by the insulation. The above figures show the results of the insulation evaluation. Two types of Kaowool insulation were investigated. One was a vacuum formed type and the other a blanket type structure. For a given thickness the vacuum formed insulation is heavier but provides lower conductivity which in turn results in a higher receiver efficiency. For either type of insulation, the insulation weight and receiver efficiency increase with increasing thickness. Therefore, as insulation thickness increases, there is an added cost for insulation and a cost savings in terms of energy cost. In addition, increased insulation weight will effect an added cost for extra support structure on the collector system. Another factor involved in the optimization is the increased solar blockage of the collector as the insulation thickness is increased. The total cost curves in the above figure are based on the cost estimates shown. The total energy cost was based on a 30 year life with 9 hour daily operation. The minimum cost for each type insulation is not significantly different. A 6 inch thickness of Kaowool vacuum formed insulation was selected for the baseline design.

The baseline receiver design concept can be summarized as follows:

Heat Exchanger

- Four (4) tube serpentine configuration
- Two (2) percent pressure loss
- 1600^{o}F peak tube temperature

Receiver

- Cylindrical shape
- 6 inches insualtion
- 8 inch diameter aperture

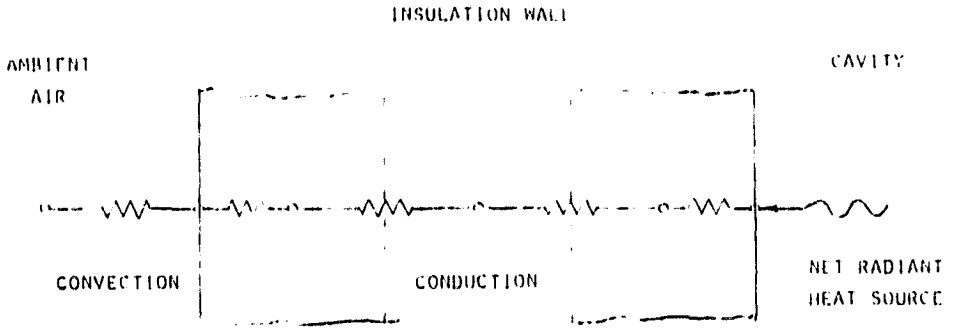

3.1.3 Thermal Model

3.1.3.1 BETA Program and Insulation Model

A detailed thermal math model was developed for the baseline receiver concept described in Section 3.1.2. This model utilizes the Boeing Engineering Thermal Analyzer (BETA) computer program along with various subroutines written specifically for the ABSR. The BETA program is used to analyze the receiver insulation and to control the overall problem analysis. The above figure shows a typical set of insulation nodes used in the BETA program. The insulation wall is broken into three internal nodes and two surface nodes at each wall location. The external surface node is coupled by convection to the ambient air node. The net radiant heat source for the internal surface node is determined by a thermal balance performed in a subroutine.

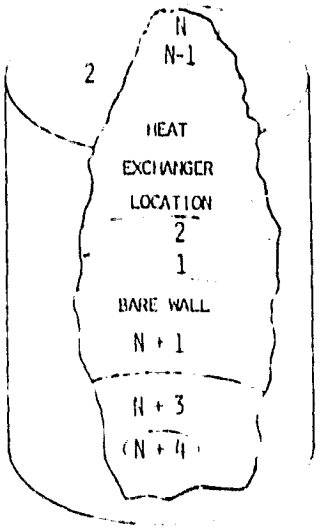

- BLACK BODY VIEW FACTOR MATRIX DETERMINED ANALYTICALLY
- SOLAR AND IR RADIATION EXCHANGE FACTOR ($\mathcal{F}$) MATRICES FOUND BY MATRIX INVERSION
- DIFFUSE RADIANT FLUX INCIDENT ON CAVITY NODE j GIVEN BY

$$\sum_{i=1}^{N+4} (\mathcal{F}_{i-j} \epsilon_i) J_i$$

3.1.3.2 Cavity Radiation Model

The internal cavity radiation exchanger factors are determined analytically in a subroutine. The cavity radiation model is shown in the above figure. The cavity sidewall is divided into nodes corresponding to each tube pass of the serpentine heat exchanger and a bare wall node (if any) located below the heat exchanger. The cavity top, bottom and aperture are also represented by individual nodes. Each material cavity node has a corresponding set of insulation nodes as shown on the previous page. The black body view factors between nodes are determined directly from the cavity geometry. The solar and infrared radiation exchange factors are determined from the black body view factors in conjunction with the cavity radiative surface properties. The diffuse radiant flux incident on each cavity node can then be found using the radiation exchange factors along with the surface self-radiosities.

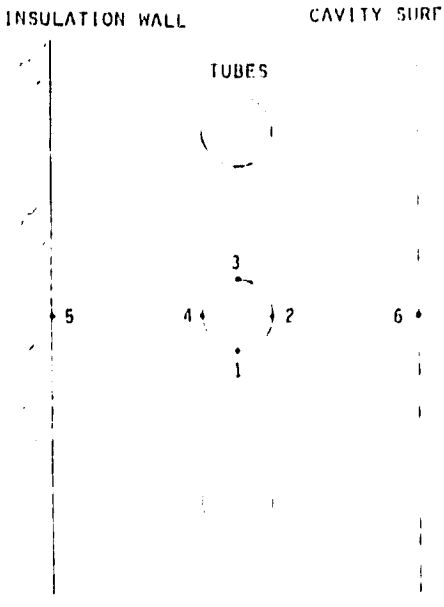

CAVITY SURFACE RADIATION
PROPERTIES DETERMINED FROM
- TUBE RADIATION PROPERTIES
- WALL RADIATION PROPERTIES
- TUBE SPACING TO DIAMETER RATIO

TECHNIQUE
- BLACK-BODY VIEW FACTOR MATRIX DETERMINED ANALYTICALLY
- SOLAR AND IR RADIATION EXCHANGE FACTOR ($\mathcal{F}$) MATRICES FOUND BY MATRIX INVERSION
- CAVITY SURFACE REFLECTANCE IS GIVEN BY

$$\mathcal{F}_{6,6}$$

- CAVITY SURFACE SELF-RADIOSITY IS GIVEN BY

$$\sum_{i=1}^{5} (\mathcal{F}_{6,i}/\epsilon_i) J_o^{-i}$$

3.1.3.3 Cavity Surface Definition

The radiative surface properties for the cavity sidewall nodes corresponding to the heat exchanger tube passes are determined in a separate subroutine. This subroutine provides a definition of the cavity surface in terms of the tube and wall radiative properties and the tube spacing to diameter ratio. The technique used in this cavity surface definition is shown in the above figure. At each cavity node location, the insulation wall, tube pass and cavity surface are represented by six nodes as shown. The black body view factors and radiation exchange factors are determined analytically. This determination then allows the cavity surface reflectance and effective surface radiosity to be found in terms of the tube/wall parameters. The insulation solar and infrared reflectivities are 0.75 and 0.63, respectively. The corresponding tube values are 0.13 and 0.17, respectively.

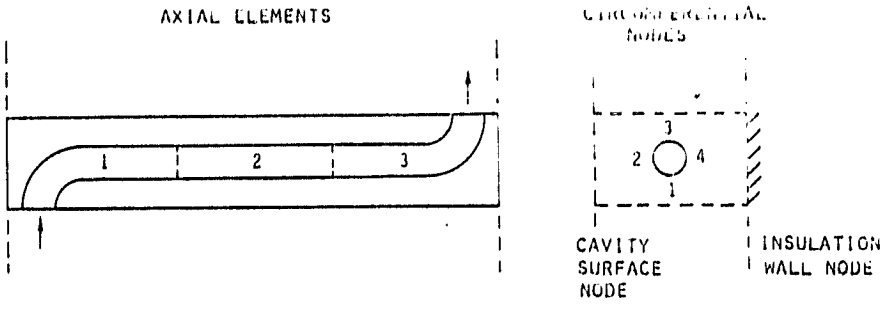

EACH TUBE PASS HAS THREE AXIAL ELEMENTS
EACH ELEMENT HAS FOUR CIRCUMFERENTIAL NODES
NUMBER OF PASSES CAN BE VARIABLE
AIR TEMPERATURE CALCULATED FOR EACH ELEMENT
EFFECTS OF BENDS INCLUDED IN HEAT TRANSFER AND PRESSURE DROP
INTERNAL TUBE RADIATION
AIR PROPERTY VARIATION WITH TEMPERATURE

3.1.3.4 Heat Exchanger Model

The heat exchanger was modeled by dividing each tube pass into three axial elements. Each of the axial elements was further divided into four circumferential nodes as shown in the above figure. For a given air inlet temperature to the heat exchanger, the heat exchanger analysis subroutine determines the air temperature at the outlet of each axial element. The convective heat transfer includes the effect of the bends and air property variation with temperature. The radiant heating of each circumferential node includes the external fluxes as well as internal tube radiation.

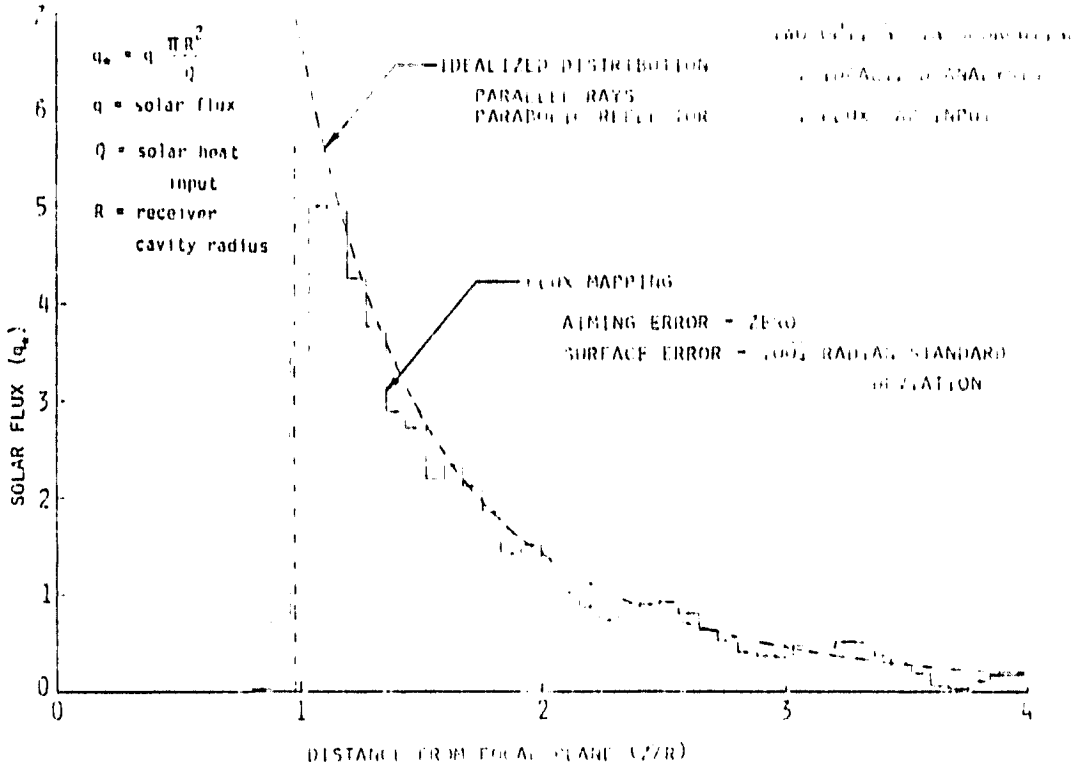

3.1.3.5 Solar Flux Distribution

Receiver performance is determined by solar flux distribution and receiver configuration. Subroutine analyses determine direct solar heating of each node based on the solar flux distribution. The direct solar flux reflected from each node is treated as a solar self-radiosity for that node. These solar self-radiosities and the infrared self-radiosities are used in the radiation exchange analyses to determine the incident diffuse flux on each node. The solar flux distribution is determined in a subroutine which has two options. One option is to input solar flux mapping data directly. The other calculates an idealized flux distribution based on a perfect parabolic collector with parallel solar rays. The above figure shows a comparison of idealized and typical flux mapping distributions. Both options give the same total flux. The major difference between them is the sharper flux peak for the idealized case. The idealized option was used for the ABSR analyses. This is a conservative approach since it results in somewhat higher peak tube temperatures.

3.1.3.6 Thermal Balance

The heat exchanger transient thermal response is found by step-wise integrations of node temperature rate of change with time. An integral number (depending on stability criteria) of integration time-steps are used within each BETA program time-step. The node temperature rate of change with time is determined at each time-step from the node thermal balance and thermal mass. The node thermal balance equates rate of heat storage to net heat input rate (i.e., absorbed radiant flux minus radiation and convection cooling).

The net radiant heating rate for each insulation interior surface node is determined by the difference in absorbed radiant flux and radiation cooling. These node heat sources are used in the BETA program to calculate the insulation node temperatures as a function of time.

HEAT EXCHANGER

TUBES (EACH CIRCUMFERENTIAL NODE)

$$\text{RATE OF HEAT STORAGE} = \text{IR HEATING} + \text{DIRECT SOLAR HEATING} + \text{REFLECTED SOLAR HEATING} - \text{RADIATION COOLING} - \text{CONVECTION COOLING}$$

AIR FLOW (EACH AXIAL ELEMENT)

$$\text{AIR HEAT GAIN} = \text{CONVECTION HEATING}$$

CAVITY

INSULATION WALL

$$\text{HEAT INPUT} = \text{IR HEATING} + \text{DIRECT SOLAR HEATING} + \text{REFLECTED SOLAR HEATING} - \text{RADIATION COOLING}$$

APERTURE

$$\text{APERTURE LOSS} = \text{IR RADIATION} + \text{REFLECTED SOLAR RADIATION}$$

NOTE: CONVECTION LOSSES THROUGH APERTURE ARE NOT INCLUDED IN PRESENT COMPUTER MODEL

3.1.3.7 Program Input and Output

The following are the program input variables:

Receiver Geometry

- Shape (cylindrical or square)
- Aperture diameter
- Insulation thickness
- Length of base sidewall

Heat Exchanger Geometry

- Number of tubes
- Number of heat exchanger tube passes
- Tube spacing-to-diameter ratio
- Tube O. D.
- Tube wall thickness
- Tube length

Radiative Properties

Thermal Properties

Boundary Conditions

- Collector focal length-to-diameter ratio
- Solar heat input to cavity
- Air mass flow rate
- Inlet air temperature

The thermal model is based on a cylindrical shape but the option exists for a more approximate treatment of a square cross-section cavity. All boundary conditions can be input as a function of time except for the collector focal length-to-diameter ratio. This ratio is used in the idealized flux distribution calculation.

The Program Output Consists Of:

Cavity Diameter and Length

Radiant Fluxes for Each Node

- Direct Solar
- Reflected Solar
- Infrared

Temperatures

- Heat Exchanger
- Air
- Insulation

Overall Thermal Balance

- Heat Input to Air
- Heat Loss Through Insulation
- Heat Loss Out Aperture

Pressure Drop

3.1.3.8 Thermal Model Summary

The thermal math model developed for the ABSR provides the means to determine the detailed thermal reponse of the selected receiver concept. The number of nodes utilized in the model is given below.

MATH MODEL NODES

Heat Exchanger	12N
Air	3N+1
Insulation	5N+15
Ambient	1

N = Number of Heat Exchanger Tube Passes

A heat exchanger with 12 tube passes results in a 257 node math model. Since the analysis is applied to only one quadrant of the receiver, this model is equivalent to a 1,025 node model of the entire receiver. In addition to providing detailed results the thermal model computer program is written in a generalized form which simplifies analyses of design variations and modifications to the program. The only significant heat transfer mechanism which is not included, in the present math model, is the convection heat loss through the aperture. An estimate of this loss is given in Section 3.1.4. The generalized form of the present model allows it to be refined to include detailed aperture convection effects when they become better understood.

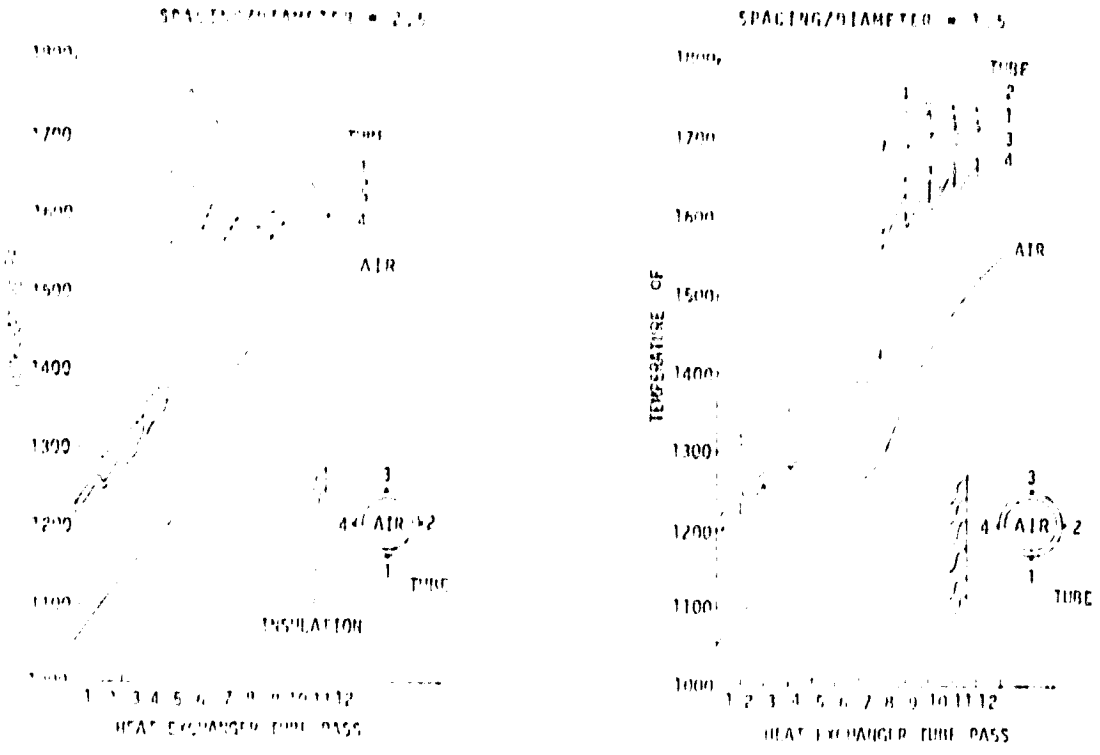

3.1.4 Thermal Analyses

3.1.4.1 Design Trades

The thermal math model described in Section 3.1.3 was used to evaluate several design trades. The comparison between cylindrical and box shape receivers, presented in Section 3.1.2.3, was one of these design trades. The math model was also used to evaluate the effect of tube spacing-to-diameter ratio. The heat exchanger temperatures for two spacing-to-diameter ratios are shown in the above figure. In both cases the heat exchanger covered the entire cavity sidewall (i.e., there was no base sidewall section). The sharp rise in tube wall temperature occurs where the tube enters the direct solar flux impingement region. These figures show that there is no undue thermal penalty for smaller tube spacings. Consequently, the tube spacing can be reduced to that compatible with mechanical design considerations. This minimizes the required cavity length. It is also apparent from the figures that the peak tube temperature is considerably higher than the 1600°F design goal.

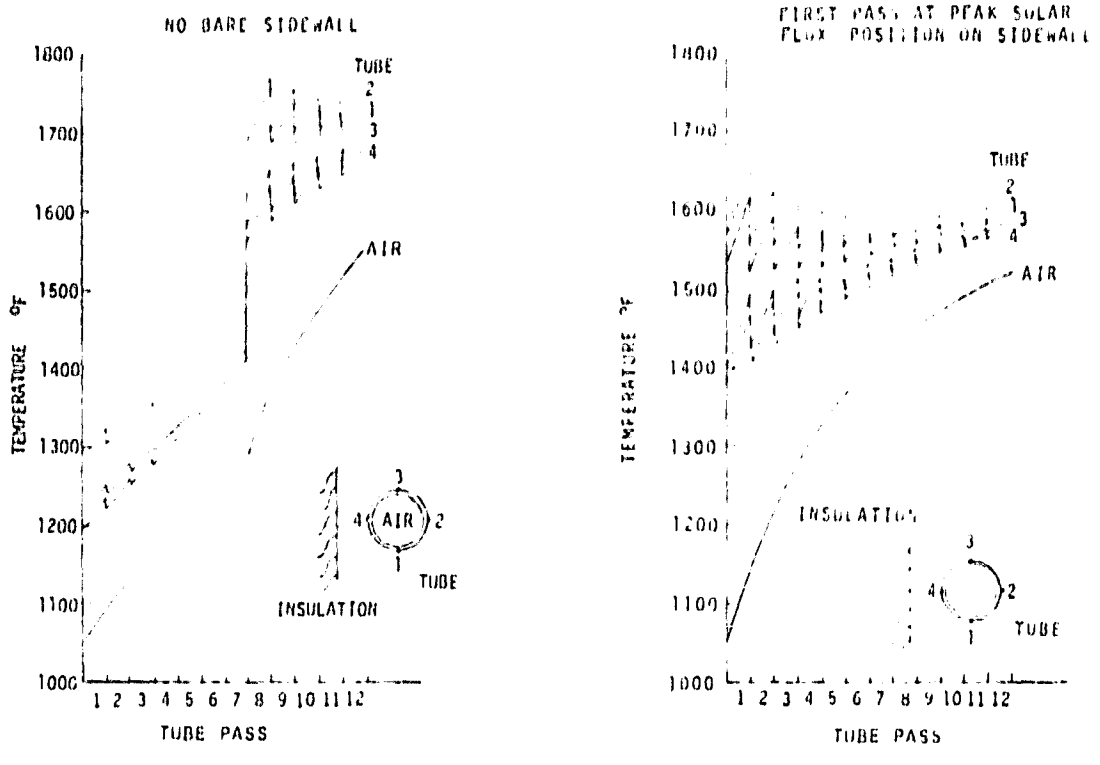

The peak tube temperature can be reduced by increasing the cavity length (i.e., by adding a base sidewall section below the heat exchanger) such that the first tube pass is at the peak flux location. The heat exchanger temperatures for this case are compared in the above figures to that of the previous case with a spacing-to-diameter ratio of 1.5. This comparison shows that the design goal peak temperature of 1600°F is nearly realized by relocating the heat exchanger relative to the solar flux distribution. This heat exchanger location was selected for the baseline design.

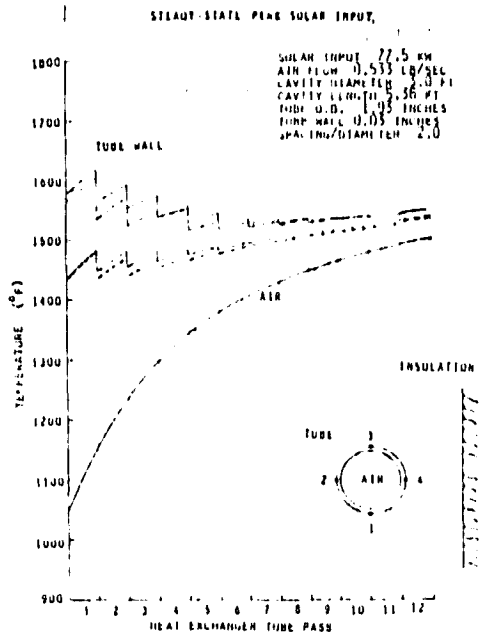

3.1.4.2 Baseline Performance Analyses

Steady-state and transient performance analyses were made for the baseline receiver configuration. The steady-state heat exchanger temperatures are shown in the above figure for peak solar heating and air mass flow rate conditions. The solar input to the cavity was reduced from the design data peak value of 85 kW to 77.5 kW. This reduction was required to keep the outlet air temperature at about 1500°F for a peak air flow rate of 0.533 lb/sec. The design point data for peak conditions implicitly assumes a receiver efficiency of about 80 percent, whereas the baseline receiver is over 90 percent efficient. Even with the reduction to 77.5 kW solar input, the air outlet temperature is still slightly greater than 1500°F. The tube temperature design goal limit of 1600°F is met in the baseline, except for a small portion of tube on the first pass where the temperature is slightly greater than 1600°F.

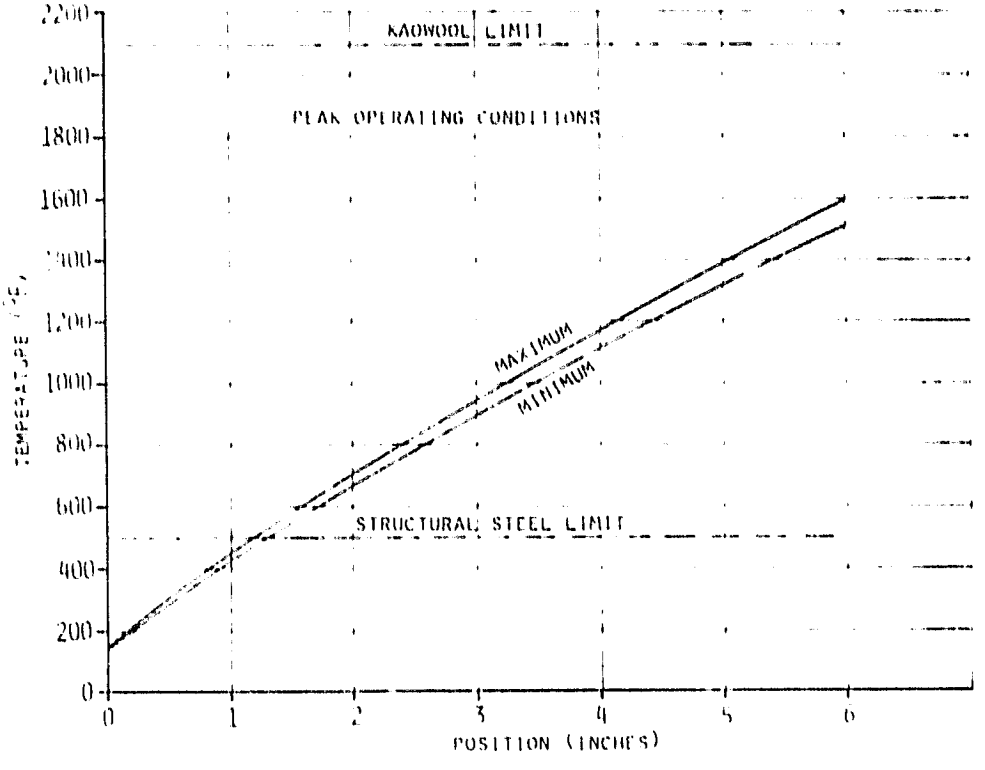

The range of insulation temperatures under peak steady-state conditions is shown above. The insulation is maintained well below the allowable Kaowool temperature limit. The external receiver temperature is also maintained well below the structural steel limit.

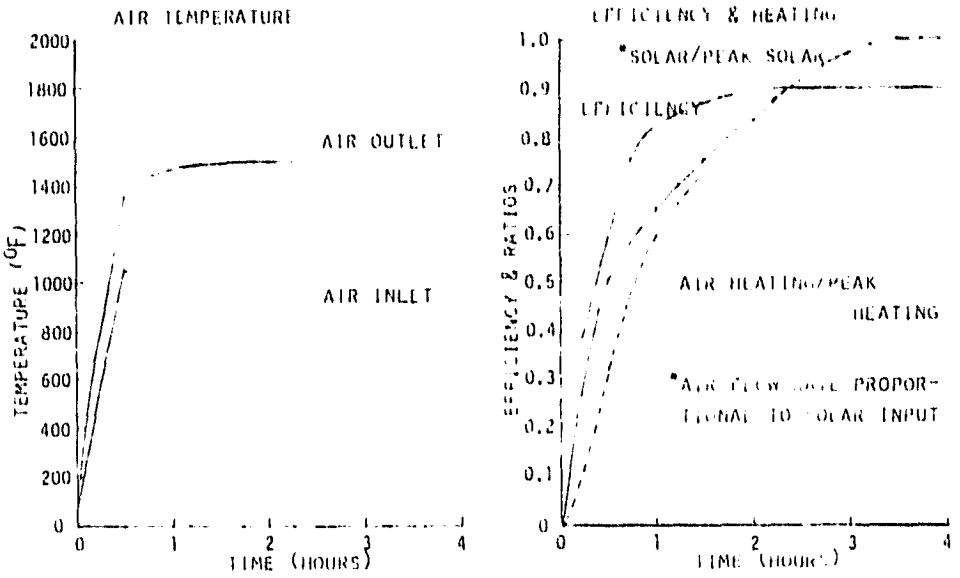

A transient analyses was made for a normal morning startup assuming the receiver to be at ambient temperature at sunrise. The startup response is shown in the above figures. The air inlet temperature to the receiver was assumed to linearly increase from ambient to 1050°F during the first half-hour after sunrise. The air flow rate was assumed to be proportional to the solar input which reaches it peak value 3½ hours after sunrise. The air outlet temperature approaches 1500°F within one hour of sunrise. Inclusion of a control value in the system would allow the outlet temperature to be maintained at 1500°F as soon as the system begins operation. The receiver efficiency approaches 90 percent two hours after sunrise. During startup the receiver efficiency is reduced because of the solar energy required to heat the receiver insulation. Analysis showed that at the end of the day, during shut-down, the efficiency remained higher than that at the start of the day since the insulation was already hot.

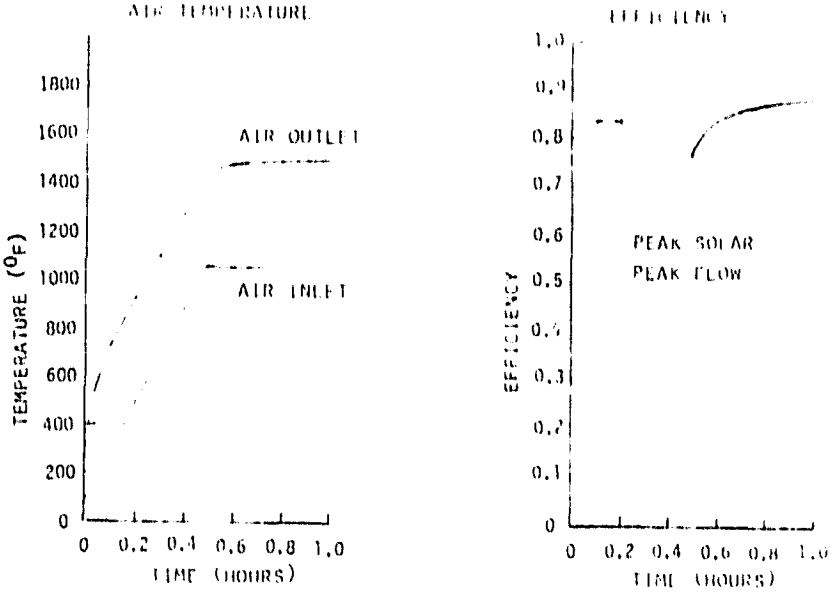

Rapid startup response was determined by starting with the receiver at ambient temperature and peak flow through the heat exchanger. At time zero peak solar input was applied to the receiver. The above figure shows the rapid startup response. As before, the air inlet temperature was assumed to increase linearly to 1050°F during the first half-hour of startup. The dashed portion of the efficiency curve covers the air inlet heat-up period. The efficiency starts at a high value and decreases during this period. This is caused by heat-up of the heat exchanger. After this half-hour period, the air inlet is held at a constant temperature and the heat exchanger temperatures are near to steady-state values. The efficiency then begins to increase as the insualtion continues to increase in temperature at an ever decreasing rate.

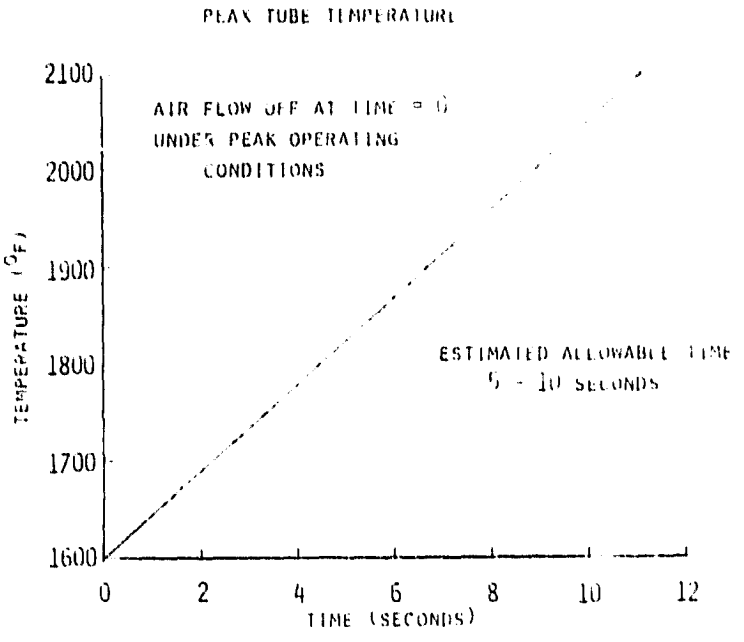

The allowable time that the heat exchanger could be exposed to peak solar flux was estimated using an approximate analysis. Since the heat exchanger tube thermal response is much more rapid than that of the insulation, it is possible to analyze the tube separately for short periods of time. Also, since the peak equilibrium tube temperature under no flow conditions is much greater than the maximum allowable tube temperature, the initial tube heating can be considered to be due to the solar flux hitting the tube. The above figure shows the initial tube temperature rise after shut-off of air flow. The primary conclusion from this analysis is that an emergency shut-down procedure is required in event of air flow shut-off.

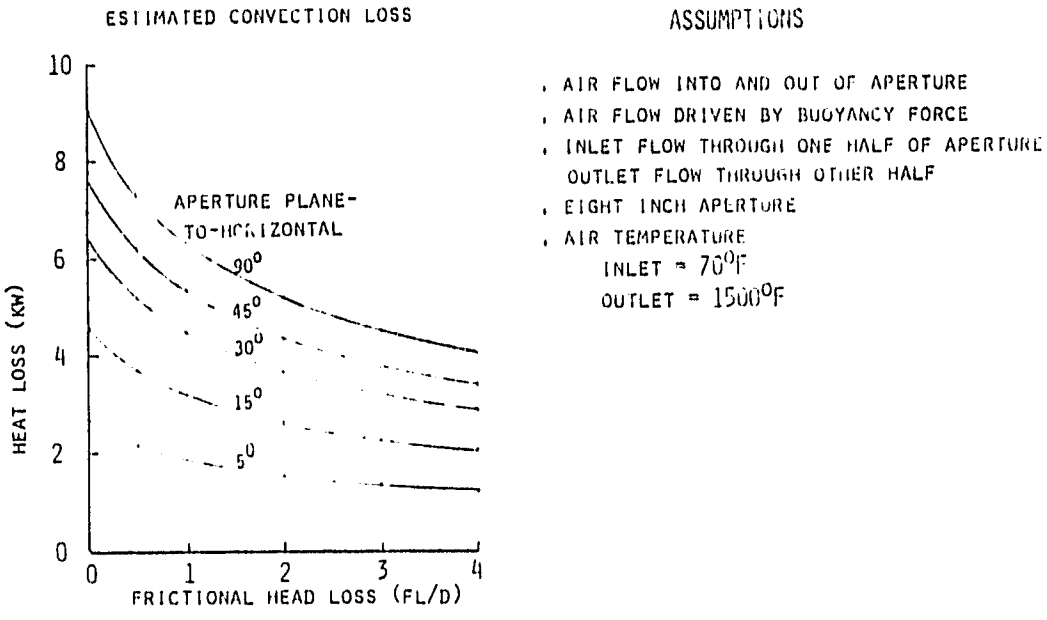

3.1.4.3 Baseline Receiver Performance Summary

Detailed thermal analysis showed the baseline receiver to have the following characteristics:

- High Efficiency
- Rapid Thermal Response
- Relatively Low Insulation and Tube Temperatures

Since the thermal math model did not include effects of convection heat lost through the aperture, these effects need to be assessed before a final evaluation of receiver efficiency can be made. A detailed analysis of aperture convection effects would be quite complex and would require experimental verification. However, an estimate of the convective loss can be made based on a simple model. The assumptions of this simple model and the estimated convection loss is shown in the above figure. This analysis shows a reasonable estimate of the aperture convection loss to be in the range of 2-8 kW.

THERMAL MODEL ANALYSIS

SOLAR INPUT TO CAVITY	77.5 KW
HEAT INPUT TO AIR	71.2
INSULATION LOSS	3.4
APERTURE RADIATION LOSS	2.9
EFFICIENCY	91.9%

The overall thermal balance for the baseline receiver design can be based in the detailed thermal analysis results in conjunction with the estimated aperture convection loss. The above table shows the thermal balance based on the detailed analysis.

REQUIRED SOLAR INPUT FOR 1500°F AIR AT 0.533 LB/SEC

HEAT INPUT TO AIR	68.5 KW
INSULATION LOSS	3.4
APERTURE RADIATION LOSS	2.9
APERTURE OVERFLOW	0.1
APERTURE CONVECTION LOSS	4-8
REQUIRED SOLAR INPUT	79-83 KW
EFFICIENCY	82.5 - 86.7%

The overall thermal balance with a 1500°F air outlet temperature and aperture convection losses is shown above. These results show that the baseline receiver design is capable of producing 1500°F outlet air at the peak flow rate with less than 85 kW solar input.

3.2 Storage

FEATURES

SENSIBLE HEAT STORAGE
350 LBS. ALUMINA SPHERES
1 INCH DIAMETER

1.1% PRESSURE LOSS AT
MAX FLOW

STORAGE FLOW SCHEMATIC

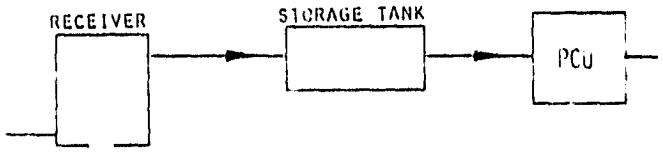

Major features of the design concept selected for the storage system are shown above. It should be noted that although the flow schematic shows the storage vessel separate from the receiver, the selected design concept has the vessel located within the receiver. The selected concept does not utilize a control valve to bypass hot air around storage. This feature greatly simplifies the design and operation of the entire system since it eliminates the valve, sensors, and control logic, and also allows the lower end of the storage tank to serve as the exhaust manifold for the heat exchangers.

The rationale and analyses that led to the selection of this concept and the size of the components are presented in the following paragraphs. Details of the pressure vessel design are given in Section 5 and the proposed assembly methods are given in Section 7.

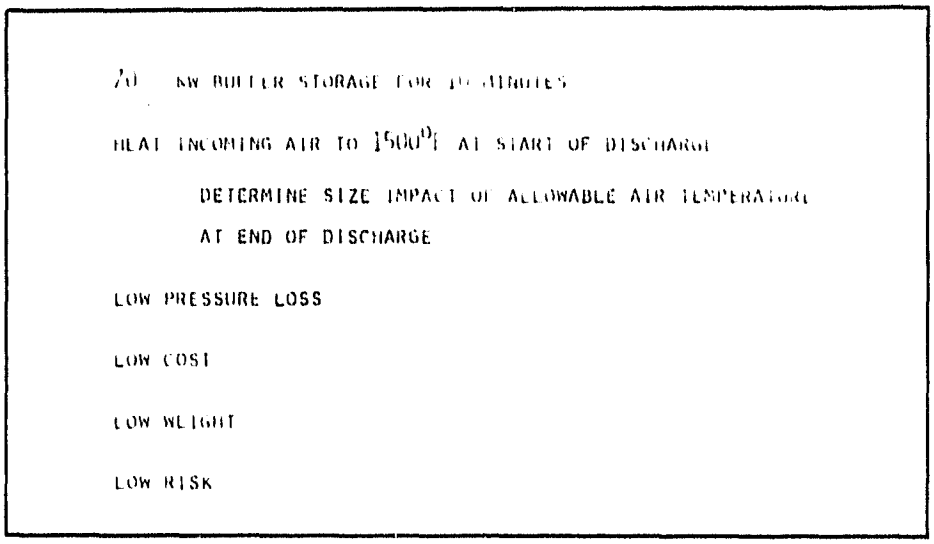

3.2.1 Requirements and Goals

The table shows the requirements and goals considered most important to the design and performance of the storage subsystem. The basic performance requirement for the buffer storage system is to provide for a 10 minute solar outage, due to cloud cover. Since the Statement-of-Work did not specify a minimum allowable value for the turbine inlet temperature (storage outlet temperature) during this time, BEC selected a minimum value of 1300°F which is reached at the end of the 10 minutes. The effect of storage media weight on the turbine inlet - time relation is shown in Section 3.2.2.5.

3.2.2 Parametric Analysis

CONCEPT	
1. STORE COMPRESSED HOT AIR	o REQUIRES 23 FT DIAMETER TANK o NOT PRACTICAL
2. REVERSIBLE CHEMICAL REACTION	
A. STORAGE BATTERY	o NOT APPLICABLE TO BUFFER STORAGE
B. THERMAL REACTION	o NOT STATE OF ART o NOT EFFECTIVE FOR SHORT STORAGE TIME
3. SENSIBLE HEAT STORAGE	o INEXPENSIVE o NO MAINTENANCE o WELL PROVEN TECHNOLOGY
4. LATENT HEAT STORAGE (LIQUID/SOLID)	o INEXPENSIVE o LIGHTER THAN SENSIBLE HEAT o TECHNOLOGY NOT PROVEN FOR THIS APPLICATION

3.2.2.1 Concept Evaluation

This table shows four concepts often considered for solar thermal energy storage. The first two concepts are impractical for application to the ABSR. Concepts three and four (sensible heat and latent heat thermal storage) are most appropriate for short term energy storage systems for Brayton cycles ("Advanced Thermal Energy Storage Systems," ERDA Contract EY-76-C-03-1300, Boeing Engineering and Construction, December 1976) and were evaluated for use in the ABSR.

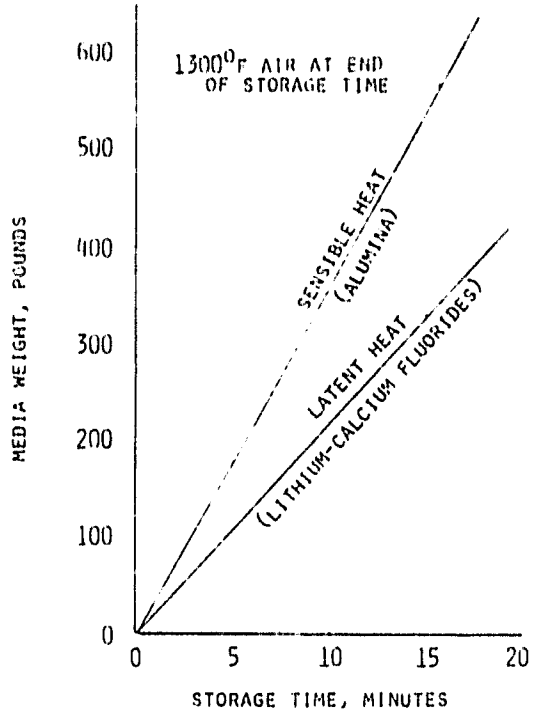

3.2.2.2 Latent Heat vs Sensible Heat Storage

The latent heat storage concept utilizes the heat of fusion associated with the phase change as the storage media solidifies during storage utilization. There are a number of chemical compounds that have a phase change temperature in the range from 1300°F to 1450°F. The most commonly suggested for use in this temperature range are mixtures of various fluoride compounds such as lithium fluoride and calcium fluoride. The design concept for latent heat systems require the use of cannisters (either evacuated or covered with an inert gas) to contain the compound and prevent direct contact with air. The cannisters are contained in a pressure vessel where the cannister surfaces exchange heat with the receiver outlet air stream.

The sensible heat storage concept utilizes materials such as refractory oxides that can be in direct contact with the air stream.

The figure shows an apparent weight advantage of approximately 130 lbs in favor of the latent heat concept. However, this does not include the weight of the cannisters required for containment of the latent heat chemicals.

	LATENT HEAT	SENSIBLE HEAT
MATERIALS	FLUORIDE EUTECTICS	REFRACTORY OXIDES
WEIGHT	≈ 22[illegible]	≈ 55[illegible]
VOLUME	[illegible] FT^3	[illegible] FT^3
COST	[illegible]	[illegible]
POTENTIAL PROBLEMS		
THERMAL EXPANSION	[illegible]	[illegible]
LONG TERM STABILITY	?	[illegible]
CORROSION	?	[illegible]
SPALLING	[illegible]	?
SELECTED FOR BASELINE		*

The table summarizes the rationale that led to the selection of the sensible heat concept. The weights are approximations of media weight only, based on a 1300^{o}F gas outlet temperature at the end of 10 minutes. The values do not include the weight of the pressure vessel, latent heat cannisters, or the necessary support and restraint structure.

The system volume requirements are essentially equal when allowance is made for the volume change associated with the latent heat phase change. Both concepts utilize commonly available materials so there is not a large cost increment.

The major difference in the concepts is that latent heat systems cannot be considered state-of-the-art for the design condition of a low cost 30 year operational life. Uncertainties regarding the thermal stability of the fluorides and the potential for corrosion of the cannisters at the high temperatures present an unacceptable design risk for the latent heat concept. The sensible heat concept presents a small risk in that the media may, over a long time, spall or give off fine dust particles. If these concerns are proven valid during the Phase II design and testing phase, low pressure drop filters can readily be installed to provide adequate protection for the power conversion system (PCU) turbine.

MATERIAL		DENSITY GMS/CC	MODULUS TO RUPTURE at 1500°F, PSI	THERMAL CONDUCTIVITY at 1500°F BTU/Hr-Ft-°F	SPECIFIC HEAT BTU/LB-°F	THERMAL EXPANSION, 10^{-6} in/in - °F between 65°F and 1500°F	RESISTANCE TO THERMAL SHOCK	RAW MATERIAL COST, CENTS/LB.	COMMENTS
ALUMINA	Al_2O_3	3.97	60K	4.6	0.29	5.0	Good	$0.41	Dust is abrasive
BERYLLIUM OXIDE	BeO	3.03	10K	10.8	0.47	4.9	Very Good	$20/lb	Potential health hazard, excessive cost
MAGNESIA	MgO	3.58	12K	4.0	0.29	7.5	Poor/ Good	$0.20/lb	Manufacturing method affects spalling resist.
SILICA	SiO_2	2.2		5.0	0.23	5.6			Severe low temperature spalling
SILICON CARBIDE	SiC	3.22	24K	12.0	0.28	2.2	ex- cellent	$1.00/lb	Excessive Cost
BORON CARBIDE	BC	2.52	40K	12.0	0.36	2.5	Good	$10/lb	Excessive Cost

3.2.2.3 Storage Media Evaluation

Desirable features of the sensible heat media include:

- o low life costs (low initial cost, no replacement or maintenance)
- o thermal stability
- o non toxic and non hazardous
- o low weight and volume (high density and specific heat)
- o adequate strength
- o proven for application (no development risks)

These requirements are met by some of the common furnace refractories. The table summarizes some of the pertinent properties of candidate materials. Of these materials, magnesia (MgO) and alumina (Al_2O_3) possess the most desirable features.

PROPERTY	STORAGE MEDIA	
	ALUMINA	MAGNESIA
APPROX WEIGHT	350 LBS	350 LBS
MEDIA COST	$ 143	$ 75
SHOCK RESISTANCE	GOOD	FAIR
THERMAL EXPANSION (R.T. TO 1500 °, 18 INCH LENGTH)	0.126 INCHES	0.19 INCHES
STRENGTH	EXCELLENT	FAIR
SELECTED FOR BASELINE	*	

This table shows that the storage media weight is the same for either magnesia or alumina. Although not shown in the table, magnesia will require approximately 11% more storage tank volume due to its lower density. Alumina is selected as the preferred material because its higher strength and better resistance to thermal shock are features that outweigh the cost increment.

The amount of thermal expansion is shown in the table to demonstrate that the relative growth of the storage media with respect to the container is not a major design concern. From room temperature to 1500^{0}F an 18 inch diameter stainless steel container will grow approximately 0.25 inches in size. Consequently, the container will accommodate the media at all temperatures and the relative movements between container and media are small.

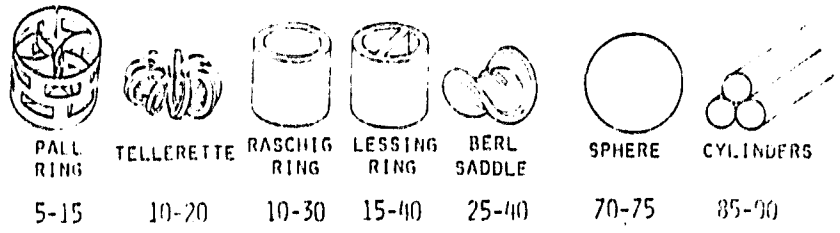

	PALL RING	TELLERETTE	RASCHIG RING	LESSING RING	BERL SADDLE	SPHERE	CYLINDERS
PACKING DENSITY	5-15	10-20	10-30	15-40	25-40	70-75	85-90

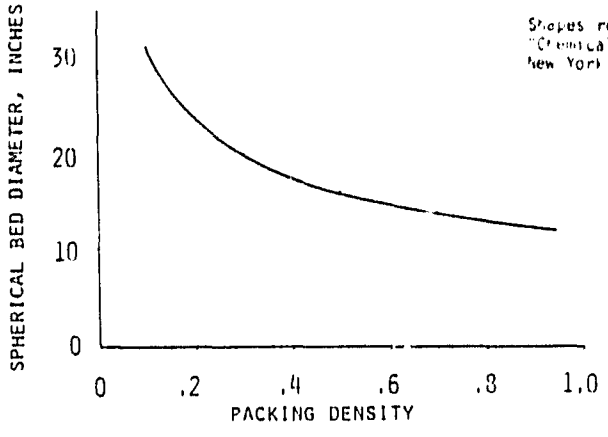

Shapes reproduced from Perry and Chilton, "Chemical Engineers Handbook," McGraw-Hill, New York, 1973, with permission of Publisher.

3.2.2.4 Media Shape Evaluation

The heat storage media must be fabricated into a shape and contained in a bed which will maximize the rate of heat transfer and minimize the pressure loss of the working fluid. Desirable characteristics of the media shape are:

- o high ratio of surface area to volume
- o low pressure loss
- o high packing density (small volume)
- o durability of shape (inherent strength)
- o low manufacturing cost
- o low installation cost

Media shapes and the associated packing density commonly used in process systems for packed columns are identified at the top of the page. The storage tank diameter (assumed spherical) required to contain 350 pounds of alumina as a function of packing density is shown in the curve.

CRITERIA	PALL RING	BERL SADDLE	PACKED SPHERES	PACKED CYLINDERS
PACKING DENSITY	POOR	POOR	FAIR	GOOD	BEST
DURABILITY	POOR	POOR	GOOD	GOOD	GOOD
RELATIVE COST	HIGH	HIGHEST	LOW	LOW	LOW
EASE OF INSTALLATION	GOOD	GOOD	GOOD	GOOD	POOR
SELECTED FOR FURTHER EVAUATION				*	*

The table summarizes the preliminary media shape selection process. The packing density criteria used in the table refers not only to the apparent density of the packed bed, but also the ability of the bed to maintain its initial volume without compaction when subjected to the anticipated vibration and motions of the storage bed mounted with the ABSR. The above evaluation shows the physical characteristics of a spherical (pebble) bed and a stacked cylinder bed are about equal and preferred over the other shapes. The next step in the shape evaluation process is to determine the pressure drop and heat transfer characteristics of the pebble and cylinder bed shapes.

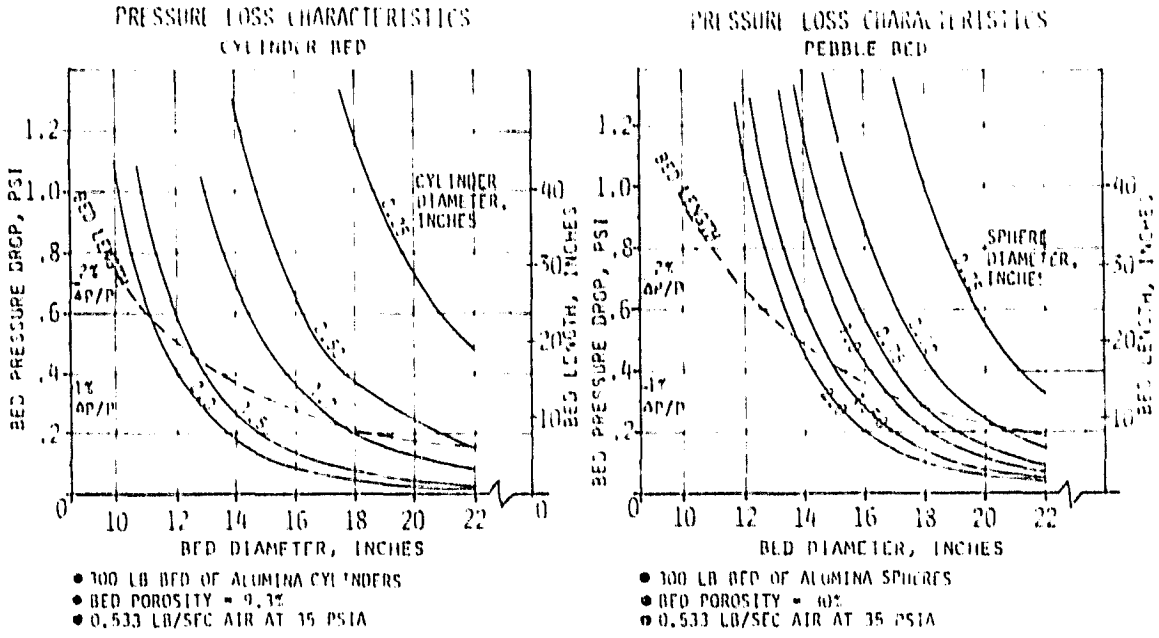

The bed pressure loss at the design rated air flow is shown in the above figures. The data is calculated from equations,(1) assuming a cylindrical bed shape. The dashed lines on the figure indicate the bed length required for a given diameter of bed to contain 300 pounds of alumina. The curves show that the pressure loss comparison can be summarized as follows:

- o low pressure loss can be attained with either shape
- o large diameter pebbles or cylinders are preferred
- o a large bed diameter with corresponding short bed length is preferred

(1) Equations are shown on the next page.

The equations for pressure drop and heat transfer in the cylinder and pebble beds were obtained from "Transport Phenomena" by R. B. Bird,et. al. John Wiley a Sons, 1960. The nomenclature employed is:

ε =void volume/bed volume
D_p = particle diameter
D_h = hydraulic diameter = 4x flow area/wetted perimeter
V_o = velocity of fluid if no particles were present
V = average velocity of fluid in bed
L = bed length
μ = fluid viscosity
k = fluid thermal conductivity
ρ = average fluid density
C_p = fluid specific heat
P_r = Prandtl number
Re_o = pebble bed Reynolds number = $\rho V_o D_p/\mu$
Re = cylinder bed Reynolds number = $\rho V D_h/\mu$
j_H = Colburn factor
$j_H = 0.91/Re_o^{.51}$ for Re_o less than 50
$j_H = 0.61/Re_o^{.41}$ for Re_o greater than 50
$4f$ = friction factor
$4f = 64/Re$ for Re less than 2500
$4f = 0.184/Re^{0.2}$ for Re greater than 2500

The pebble bed pressure loss is:

$$\frac{\Delta P}{L} = \frac{150\mu V_o (1-\varepsilon)^2}{D_p^2 \varepsilon^3} + \frac{1.75\rho V_o^2 (1-\varepsilon)}{D_p \varepsilon^3}$$

The pebble bed heat transfer coefficient is:

$$h = 6 j_H C_p \rho V_o (1-\varepsilon) Pr^{-2/3}$$

The cylinder bed pressure loss is:

$$\frac{\Delta P}{L} = \frac{4f \rho V^2}{D_h \; 2g_c}$$

The cylinder bed heat transfer coefficient is:

$$h = 0.023 \frac{k}{D_h} Re^{.8} Pr^{1/3} \quad \text{for Re greater than 2300}$$

$$h = \frac{k}{D_p}\left[4 + 0.16\left(\frac{D_h RePr}{L}\right)^{3/4}\right] \quad \text{for Re less than 2300}$$

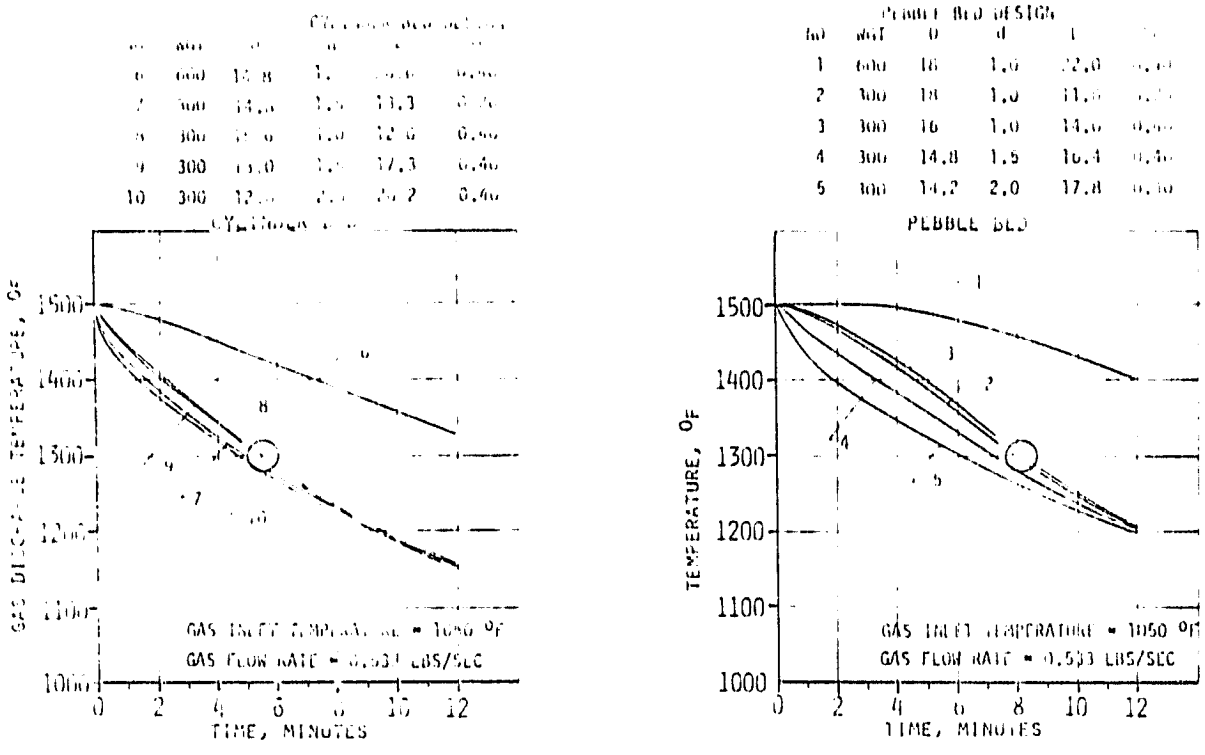

D = BED DIAM., INCHES L = BED LENGTH, INCHES
d = PARTICLE DIAM., INCHES ΔP = BED PRESSURE LOSS, PSI

The discharge temperatures shown above were calculated with the BETA program (see paragraph 3.1) utilizing 21 nodes for the air stream and 20 nodes for the storage media representation. The curves are labeled to identify parameters shown at the top of the page. Bed diameters were selected to allow a direct comparison based on bed pressure loss.

If a 1300°F minimum allowable discharge temperature is assumed, the data show a 300 pound pebble bed provides up to eight minutes of storage while a cylinder bed of the same weight and pressure loss provides only 5½ minutes of storage. The 30 percent longer storage time is a consequence of the higher values of convection coefficient and wetted area inherent in pebble beds.

A comparison of curves 3, 4 and 5 show that, for the same pressure loss, small diameter spheres increase the thermal performance. However, as shown previously small diameter spheres require increased bed diameter and decreased bed length to minimize pressure loss. Stipulating that the bed length-to-diameter ratio should not be less than 1 (to minimize the potential for flow stratification or channelizing within the bed) fixes the sphere size at approximately 1 inch. This is a commonly mass produced size.

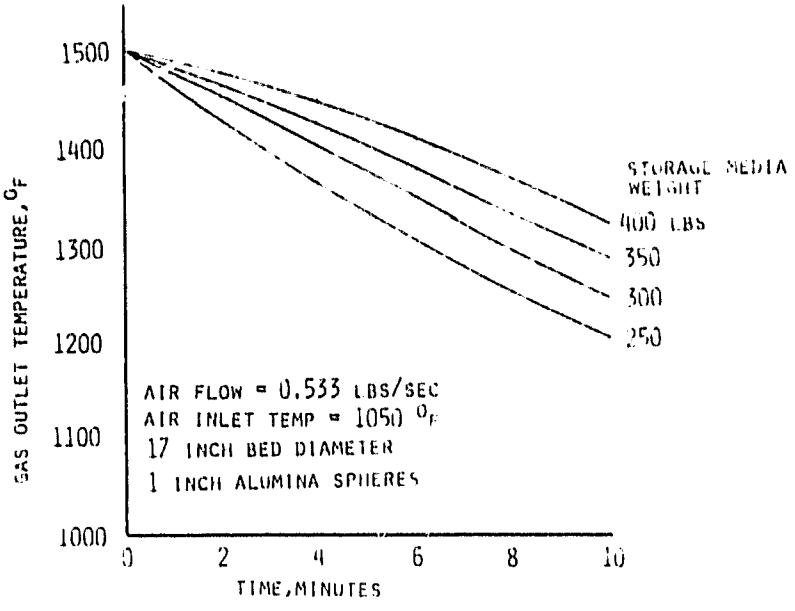

3.2.2.5 Storage Media Weight Evaluation

This figure shows the effect of changing bed length (and pressure drop) to accommodate a variable quantity of storage media. Bed diameter was constant at 17.2 inches based on using an 18 inch standard pipe size for the storage tank. The bed pressure drop scales linearily with bed weight in this case, varying from 0.19 psi at 250 pounds to 0.31 psi at 400 pounds bed weight. The storage system weight selected for the conceptual design is 350 pounds which gives a bed pressure loss of 0.27 psi.

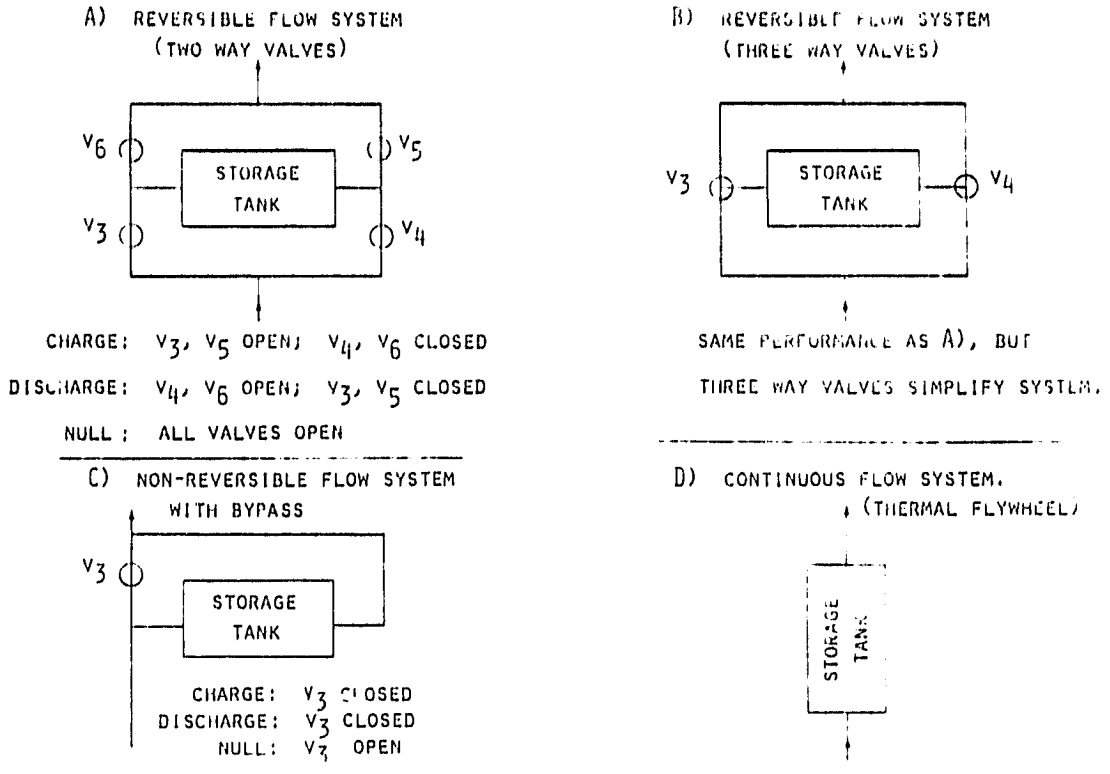

3.2.2.6 Storage Flow Control Evaluation

Four methods of controlling the air flow through and around storage are shown above. Concept D, the thermal flywheel, is the simplest since it involves no controls or sensors. It penalizes the system because it provides a continuous pressure loss. There may be a small system penalty since PCU inlet temperature cannot be controlled it depends only on the recent thermal history of storage.

Concept C uses a bypass valve to divert air around storage to minimize pressure loss when storage is not utilized. If the valve has a positioner, it can modulate flow to supply the most desirable mixture of receiver and storage outlet temperatures to the turbine.

Concepts A and B are refinements of concept C which allow reversed flow through storage. This is advantageous when energy from storage must be utilized when storage is not completely charged. Reversing the flow makes efficient use of bed thermoclines to supply the highest storage outlet temperature.

The evaluation process for these concepts is a cost versus benefit procedure. The first step is to determine the apparent cost penalty of the continuous pressure loss inherent in concept D.

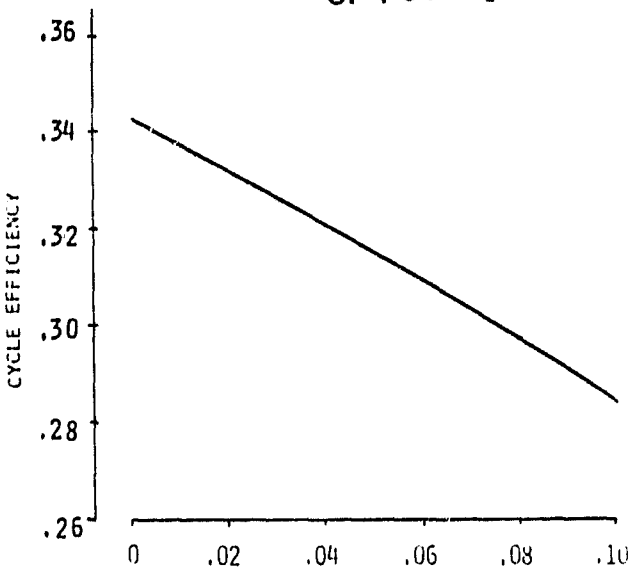

$$\eta_c = 1 - \frac{\frac{r_p^{\delta} - 1}{\eta_b} + \frac{T_4 - T_2}{T_o}}{\frac{T_3}{T_o}\eta_T\left[1 - \left(\frac{G}{r_p}\right)^{\delta}\right] + \frac{T_4 - T_2}{T_o}}$$

r_p = pressure ratio = 2.5
η_b = compressor efficiency = 0.796
η_t = turbine efficiency = 0.872
T_o = compressor inlet temp. = 80°F
T_2 = receiver inlet temp. = 1050°F
T_3 = receiver outlet temp. = 1500°F
T_4 = turbine outlet temp. = 1177°F

$$G = \frac{1}{\left(1 - \frac{\Delta P_1}{P_1}\right)^2 \left(1 - \frac{\Delta P_s}{P_s}\right)}$$

$\frac{\Delta P_1}{P_1}$ = recuperator pressure loss, each pass = .0265

$\frac{\Delta P_s}{P_s}$ = receiver/storage pressure loss, parameter

γ = specific heat ratio = 1.342

$\delta = \frac{\gamma - 1}{\gamma}$ = .2548

(NOTE: Curve in Final Technical Report is in error)

The above chart shows the effect of pressure loss on thermodynamic cycle efficiency of the turbine/compressor unit. It is important to note that the magnitude of cycle efficiency shown above is not used in the following analysis; only the slope is important. The slope is essentially constant at 0.57% cycle efficiency loss per 1% increase in pressure loss.

If 68KW thermal input to the PCU yields 16.75 KW electrical when the receiver/storage pressure loss is X percent, then the same thermal input combined with a pressure loss of X + 1 percent yields an electric output of 16.45KW.

Assuming the energy can be sold for 50 mills per KW-hr, a 30 year life at 8 hours per day gives a simple revenue loss of $1300. A present value cost analysis based on a 5% inflation rate shows the 30 year energy loss has a present value of $670.00.

Based on these simple calculations, it can be concluded that it is definitely not cost effective to spend more than $1300 to bypass the storage system; the break-even point is expected to be considerably lower.

COST BASIS:

- 4 INCH BALL VALVE
- 600 POUND ANSI RATING
- HIGH TEMPERATURE VERSION OF A STANDARD VALVE
- PNEUMATIC ACTUATOR AND POSITIONER

	COST PER VALVE * ANNUAL PRODUCTION			
	100	1000	10,000	100,000 OR MORE
BASIC VALVE	$ 2890	$ 2170	$ 2170	SPECIAL PRODUCTION FACILITY WILL REQUIRE RESTRUCTURED PRICING
VALVE AND ACTUATOR LESS POSITIONER	$ 2560	$ 1920	$ 1920	

* VALVE COST QUOTATION, KAMYR VALVE COMPANY

Valve costs as a function of production rate are shown in the above table. As indicated, the costs are based on a slight modification of a current product line and, therefore, are realistic. The price of the basic valve includes the position transducer which allows the valve to modulate flow. The lower line of cost data applies to an open-shut valve only.

Conversations with the valve vendor revealed that one three-way valve will cost more than two of the two-way valves which it replaces, but there could be a slight weight reduction.

	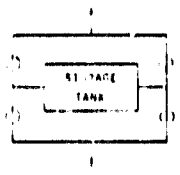	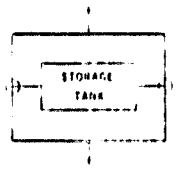		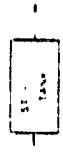
THERMAL PERFORMANCE NULL IN USE	GOOD BEST IF STORAGE MUST BE USED PRIOR TO FULL CHARGE	GOOD	GOOD GOOD	GOOD GOOD
CONTROL	BEST	BEST	GOOD	NONE
PRESSURE LOSS NULL IN USE	0 EXTRA BEND LOSS	0 EXTRA BEND LOSS	0 LOW	LOW LOW
APPROXIMATE VALVE COSTS	$11,000	> 11,000	$2,000	0
SELECTED FOR BASELINE				X

The results of the valve cost analyses summarized above are based on moderate production rates; the conclusions are considered valid at other production rates.

Since the reversible flow systems have better performance only when storage is used prior to a fully charged condition, the cost of the extra valves cannot be justified.

Based on a 1% storage system pressure loss, the present value of electricity saved by a bypass valve is less than $700. Since the valve cost (not including maintenance) exceeds the potential savings, the continuous flow system is preferred at this time. However, the final decision must be based on minimum energy costs over the system life. Factors which have not been included in the above analysis may be important. Some factors such as system operating strategy and turbine performance when operating with low inlet temperature may increase the desirability of installing a bypass valve. On the other hand, the interaction of valve dynamics with PCU dynamics and rapid fluctuations in the solar flux increase the desirability of the continuous flow system (fixed flow resistance). These factors must be considered in the final design to insure that the selection is correct.

THERMAL FLYWHEEL CONCEPT	NO VALVES REQUIRED
BED MATERIAL	ALUMINA SPHERES
BED WEIGHT	350 LBS
BED DIAMETER	17.17 INCHES
BED LENGTH	14.2 INCHES
BED ΔP AT MAXIMUM FLOW	0.77%
TOTAL ΔP AT MAXIMUM FLOW (INLET-TO-OUTLET)	1.12%
SPHERE DIAMETER	1 INCH
NUMBER OF SPHERES	4,650
TOTAL WETTED AREA	101 FT^2

3.2.2.7 Storage Conceptual Design Summary

This table summarizes the selected concept for the thermal storage system. Bed diameter was selected on the basis of installing the pebbles inside of an 18 inch diameter standard pipe with an allowance for lining the pipe with 1/4 inch of compressible packing to prevent flow channelization around the edge of the bed.

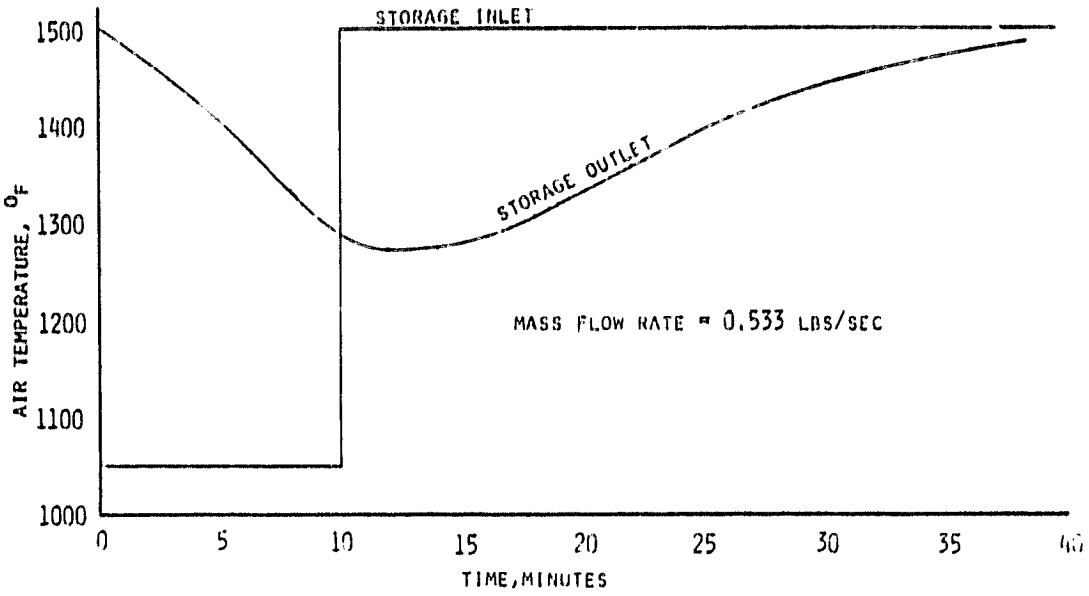

3.2.3 Performance of Selected Design

3.2.3.1 Temperatures, Discharge and Recharge Cycle

The figure shows the air temperature leaving storage during, and for 30 minutes following a solar outage. At time zero, the bed is uniformly at 1500°F and the inlet air temperature is dropped to 1050°F. The step change is a reasonable approximation of the receiver outlet temperature following a cessation of solar flux. However, other assumptions used as boundary conditions in the analysis are overly simplified since neither air flow rate nor inlet temperature will remain constant during discharge. The computer model utilized to represent the storage system is capable of utilizing time or temperature dependent boundary conditions when they are better defined.

Under the assumed conditions the storage system provides 10 minutes during which time the gas outlet temperature remains above 1300°F. The outlet temperature continues to decrease for two minutes after the inlet temperature increased to 1500°F because of thermoclines existing in the storage bed.

The analysis shows that storage is essentially fully charged (1450°F gas outlet temperature) within 20 minutes after the increasing inlet temperature. Temperature profiles of the storage media are shown on the next page.

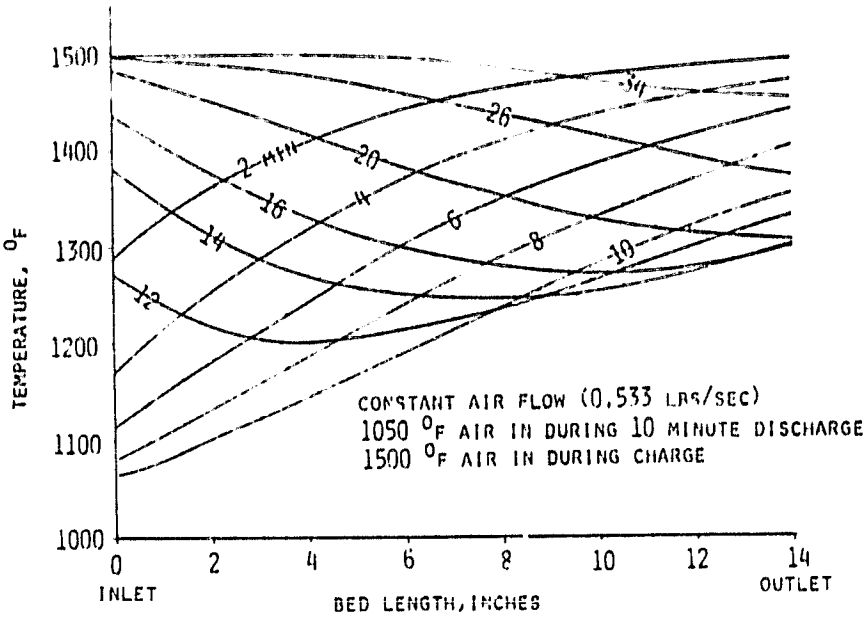

Bed temperature profiles during the discharge and recharge cycle are shown on the figure. The curves' labels are time in minutes. Curves labeled 2 through 10 show the bed temperature at the indicated time during the 10 minute discharge period. The curves labeled 12 through 34 show the bed temperature profiles during the recharge period.

The previous page showed that gas outlet temperature continued to decrease for approximately 2 minutes after the inlet temperature was increased. The reason this happens is clear when the 10 minute through 14 minute thermoclines are examined.

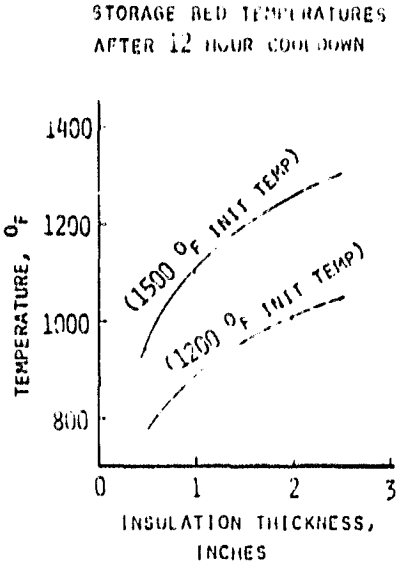

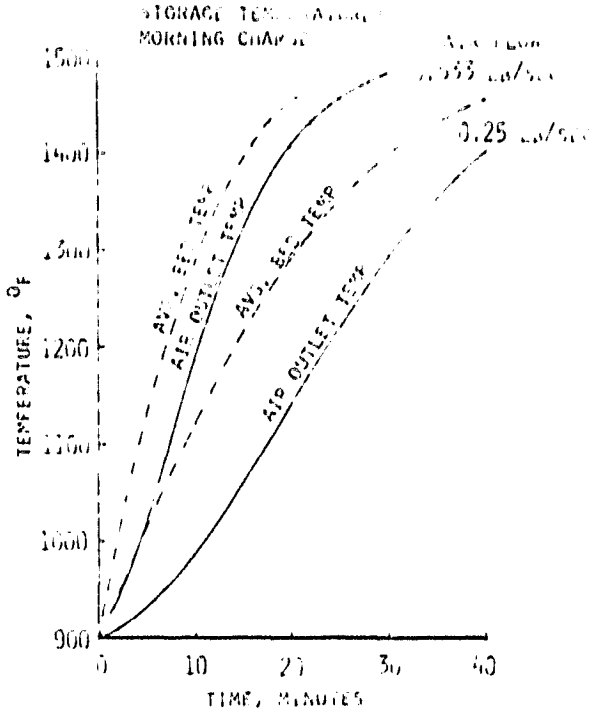

3.2.3.2 Warmup From Overnight Cool-down

The figure on the left shows bed temperatures after 12 hours of overnight cooling as a function of storage tank insulation thickness and bed temperature at the start of the cooling period. The data assumes that the storage tank is located inside the receiver so some benefit is derived from the receiver thermal insulation.

If the tank were located outside the receiver, insulation thickness would have to be approximately 3 inches thicker to achieve the same overall effect. On the basis of this data and the amount of space available inside the receiver, an insulation thickness of 1 inch was selected.

The curve on the right shows the morning warm-up response of the storage bed for two different air flow rates assuming a 1500°F inlet air temperature. As a point of interest, the mass average bed temperatures are plotted as dashed lines. The curves show that with full flow rate, bed warm-up can be achieved in 25 minutes (1450°F air outlet temperature).

DISCHARGE TIME	10 MINUTES (1300°F AIR OUTLET)
RECHARGE TIME	20 MINUTES (1450°F AIR OUTLET)
TEMPERATURE AFTER 12 HOUR COOLDOWN	900°F
TIME REQUIRED FOR MORNING RECHARGE	25 MINUTES (1450°F AIR OUTLET)

3.2.3.3 Storage Performance Summary

The above table summarizes the thermal performance characteristics of the 350 pound alumina pebble bed storage system. As shown in paragraph 3.2.2.7, the bed has a maximum end-to-end pressure loss of 1.1 percent.

4.0 Functional Interfaces

COMPONENT	AVERAGE VELOCITY FT/SEC	PRESSURE LOSS, PERCENT
INLET FLANGE	62	0.01
MANIFOLD	62	0.11
HX INLET	62	0.20
HX	135	2.0
EXPANSION TO STORAGE	135	0.30
BED LOSS	17	0.80
CONTRACTION TO OUTLET	81	0.05
OUTLET FLANGE	81	0.02
	TOTAL	3.5 PERCENT

4.1 PRESSURE LOSS

The sources of all pressure loss within the BEC Air Brayton Solar Receiver and storage system are identified above. The baseline system has no moving parts or valves so the pressure loss will be only a function of the square of the mass flow rate divided by the average air density within the receiver/storage unit.

The ability to achieve low pressure loss without requiring valves greatly enhances system performance because it simplifies the control system logic and eliminates any possibility of flow instabilities caused by the response characteristics of the PCU system acting in opposition to variable flow characteristics of the receiver system.

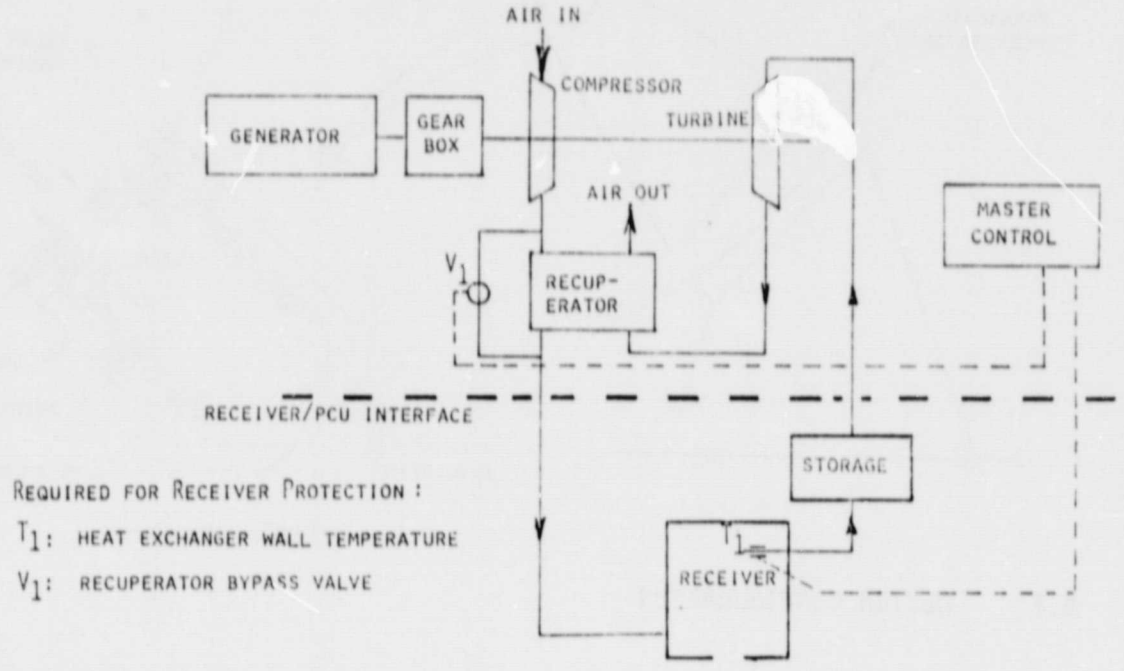

4.2 FLOW SCHEMATIC AND CONTROLS

The above diagram shows the Receiver/PCU interface and the sensors and controls required to protect the receiver. T_1 represents temperature sensors located on the heat exchanger tubes. It is anticipated that these signals will be supplied to a Master Control System which commands valve V_1 to bypass a portion of the compressor outlet air around the recuperator whenever any of the T_1 signals exceed the tube design rated temperature ($1600^{o}F$). The decrease in receiver inlet air temperature will adequately protect the receiver and heat exchanger tubes provided a minimum of air flow is maintained.

If the even air flow to the receiver is stopped, the Master Control System must command concentrator slewing when the T_1 signals exeed approximately $1700^{o}F$.

5.0 Design Description

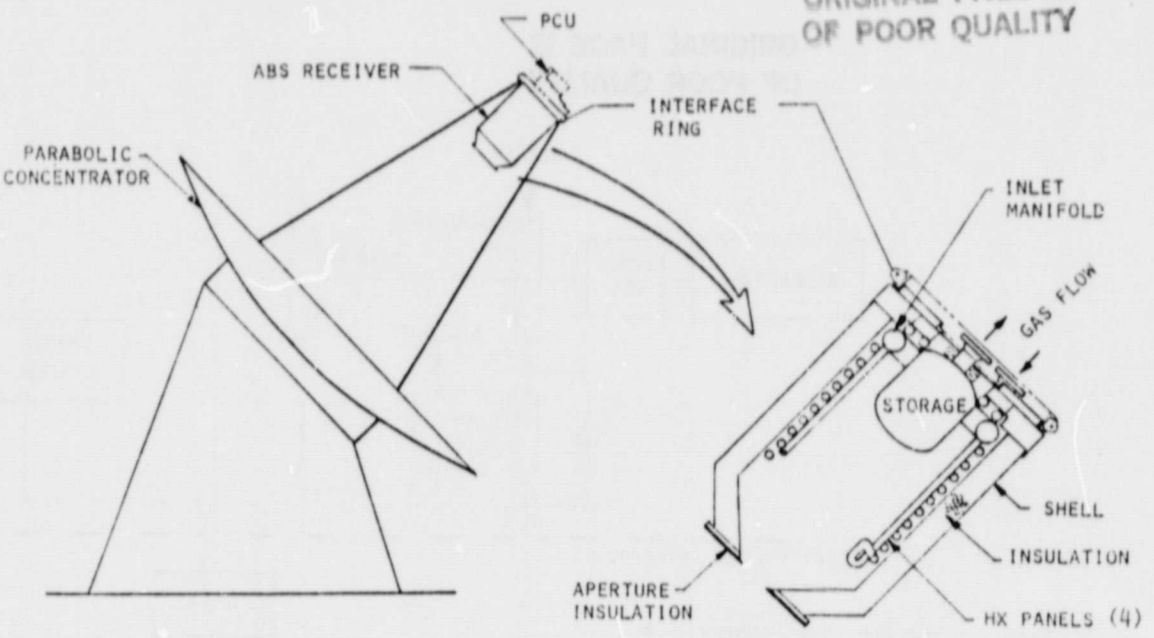

RECEIVER COMPONENTS

5.1 DESIGN CONFIGURATION

The ABSR conceptual design configuration shown above has been designed for high efficiency, and a conservative design approach not only meets the 30 year design requirement, it requires no planned maintenance during its life. The ABSR design meets or exceeds the following design requirements.

- LOADS
  - SEISMIC
  - WIND
  - TRANSPORTATION
  - GRAVITY

  } ASSUME 3 G WORST CASE
- THERMAL
  - BUFFERING - 10 MIN. TO 1300°F
  - TEMPERATURES:
    - GAS INLET 1050°F
    - GAS OUTLET 1500°F
    - Hx TUBING 1600°F
- HEAT TRANSPORT FLUID
  - RECEIVER INLET 35 PSIA
  - MASS FLOW 0.533 LB/SEC
  - PRESSURE DROP 4% MAXIMUM
- CONFIGURATION
  - MINIMIZED ENERGY COST - SIZE, APERTURE, INSULATION THICKNESS
  - C. G. NEAR INTERFACE RING
  - INDEPENDENT INSTALLATION/REMOVAL
  - ENVIRONMENTAL PROTECTION
- LIFE - 30 YEARS

	MATERIAL	EXPERIENCE/RATIONALE
Hx Tubing	INCONEL 617	DEVELOPMENT TESTS: THERMAL CYCLING WELD JOINTS APPLICATION: BENCH MODEL SOLAR RECEIVER
Inlet Manifold & Storage Vessel	18 - 8 S. S.	ASME CODE ACCEPTANCE, COST & AVAILABILITY
Cavity Insulation	B & W KAOWOOL PRODUCTS	LAB TESTS: SPECTRAL PROPERTIES SOLAR FLUX EXPOSURE APPLICATION: BENCH MODEL SOLAR RECEIVER
Aperture Face Insulation	KAOWOOL 3000 BOARD + ZIRCONIA BOARD	LAB TESTS: SOLAR TO 3700 KW/m^2 @ WHITE SANDS APPLICATION: BENCH MODEL SOLAR RECEIVER
Storage Media	ALUMINA SPHERES	COMMON USEAGE IN PEBBLE BED HEATERS

5.2 MATERIAL SELECTION

The Table summarizes the design material selection and the rationale for the selection. The following paragraphs present some of the background experience that BEC has with these materials.

	INCONEL 617	HS 188
100,000 STRESS-RUPTURE (1600°F)	- C O M P A R A B L E -	
BOEING TESTS	30 YRS. DIURNAL CYCLING THERMAL CYCLING TO RUPTURE	
WELD DRAWN TUBING	SPECIAL ORDER (SUPERIOR TUBE)	SPECIAL ORDER (CABOT CORP.)
DESIGN/FABRICATION/TEST EXPERIENCE	BOEING/EPRI BENCH MODEL SOLAR RECEIVER	
COST & DELIVERY	- C O M P A R A B L E -	
WELDABILITY	GOOD	GOOD - LIMITED EXPERIENCE
INSPECTION	CONVENTIONAL TECHNIQUES . X-RAY . PENETRANT	SPECIAL PRACTICE X-RAY

5.2.1 High Temperature Materials

BEC recently conducted an industry wide assessment of metal alloys suitable for use in oxidizing atmospheres at temperatures in the 1400 to 1800°F range. The prime requirements were: low oxidation rate, high creep rupture strength, and availability. Two candidate materials were far superior to all others: Inconel 617 (Huntington Alloys) and Haynes 188 (Cabot Corporation). The table shown above compares these alloys.

The table indicates that the materials are essentially equal in all respects except Haynes 188 requires a special X-ray technique fo weld inspection due to the tungsten content. Inconel 617 was selected for use in the EPRI Bench Model Receiver mainly on the basis of current availability at the time the order was placed.

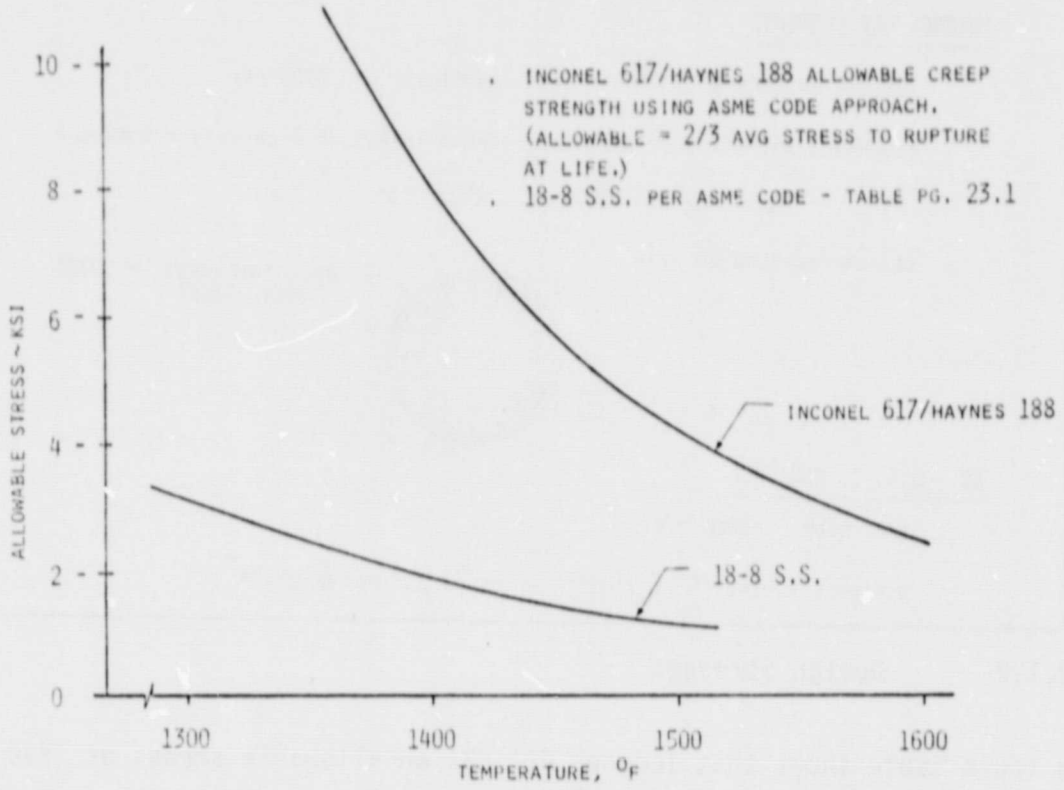

5.2.1.1 Material Allowable Stresses

The above figure shows the allowable stress versus temperature based on the ASME code procedure of using the lesser value of 1/2 of tensile strength or 2/3 of average stress to creep rupture at 100,000 hours.

The 18-8 stainless curve is an actual ASME allowable for 304 stainless to 1500°F. The values shown for Inconel 617 and Haynes 188 are not ASME approved, but are obtained by using Larson-Miller extrapolation of 1 to 10 thousand hour creep-rupture test data to obtain 100,000 hours values and applying the ASME approach to obtain an allowable stress.

INCONEL 617 ELEMENTS

. 100,000 HR LIFE @ 1600°F, STRESS - RUPTURE = 3800 PSI

. ALLOWABLE PRIMARY PLUS SECONDARY STRESS (PRESSURE + GRAVITY + THERMAL)

$S_M = 2/3 \times 3800 = 2530$ PSI

. DESIGN PRESSURE 20 PSIG

18 - 8 S. S. MANIFOLD

. ANSI CODE - POWER PIPING

. SCHEDULE 5 PIPE (5" x .109") - RATED 237 PSI @ 1050°F

5.2.1.2 Design Stresses

The above table shows that Inconel 617 has an allowable stress of 2530 psi at the design temperature of 1600°F. If the only consideration were pressure induced stresses, a wall thickness of 0.008 inches would be adequate for the heat exchanger tubes. However, the additional stresses imposed by

- temperature gradient along the tube length,
- temperature gradient around tube perimeter, and
- gravity, seismic, and vibration (3 g assumed)

dictate a thicker wall section. Preliminary stress analyses indicate that an 0.028 inch wall thickness will provide adequate strength.

The inlet manifold will be exposed to 1050°F air (it is insulated from the cavity environment) for most of the design life. During startup and part power operation conditions it can contain 1320°F air. The manifold is not subjected to thermally induced stresses but it must support itself and the heat exchangers for the gravity, seismic, and vibration loads. Preliminary stress analyses indicate a 5 inch diameter schedule 5 pipe (304 stainless steel) has adequate strength to meet the ANSI power piping code requirements.

- HUNTINGTON ALLOYS/BOEING AGREEMENT
  - PIPE AND TUBE, SEAMLESS OR SEAM WELDED

CHEMICAL COMPOSITION (%)

NI	44.5 MINIMUM	SI	1.0 MAXIMUM
CR	20-24	MN	1.0 MAXIMUM
CO	10-15	S	.015 MAXIMUM
MO	8-10	CU	0.5 MAXIMUM
FE	3.0 MAXIMUM	B	.006 MAXIMUM
AL	0.8-1.5	C	.05-.15
TI	0.6 MAXIMUM		

MECHANICAL PROPERTIES

MINIMUM RT TENSILE	90,000 PSI
MINIMUM RT YIELD	30,000 PSI
ELONGATION (2-IN.)	35%
MINIMUM STRESS RUPTURE LIFE	24 HOURS @ 1,600°F = 14,000 PSI

  - CONDITION - ANNEALED
  - FINISH - PICKLED

5.2.1.3 Selection - Heat Exchangers

The table summarizes an agreement reached between Boeing and Huntingtom Alloys for the composition and properties of Inconel 617. This agreement is in the process of becoming a formal specification.

BEC proposes to use Inconel 617 as the heat exchanger material for the ABSR because of the favorable Bench Model fabrication and test experience, the ease of weld inspection, and the near complete status of the material specification.

	18-8 S.S.	INCONEL 617
SUITABLE FOR 1500°F SERVICE - 30 YR	YES	YES
DESIGN CRITERIA	ASME CODE	CREEP - RUPTURE
MATERIAL COST/EACH	$350	$1575
FABRICATION	- COMPARABLE FORMING & WELDING -	
AVAILABILITY	OFF THE SHELF	DEPENDS ON PRODUCTION QUANTITY
ATTACHMENT TO IIx	WELD - TESTS REQ'D ALT: BRAZE, DIFFUSION BOND	WELD

PREFERRED

5.2.1.4 Material Selection - Storage Vessel and Inlet Manifold

The storage vessel and inlet manifold are covered with 1 inch of Kaowool insulation to provide protection from the receiver cavity thermal environment. The elimination of the thermal gradient stresses allow the use of stainless steel for these components.

The above table summarizes the trade study made to determine the preferred material. As indicated, the use of stainless greatly reduces the raw material cost and the greater availability will tend to reduce the fabrication costs. However, the ability to weld the Inconel heat exchangers to a stainless manifold and receiver has not been demonstrated. Boeing metallurgists indicate there should be no problem in welding based on the similarity of constituents but this area will require further investigation and test. If the weld technique does not prove out, alternate attachment methods such as nickel brazing or diffusion bonding are acceptable alternates.

- FLUX DISTRIBUTION - NORMAL USE
  (SLOPE & TRACKING ERRORS)

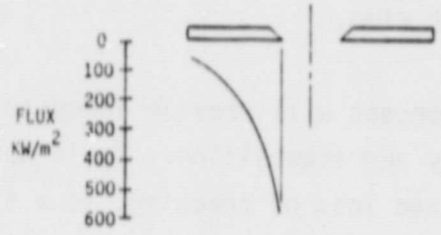

- FLUX DISTRIBUTION MID-DAY STARTUP
  (SLOPE ERRORS)

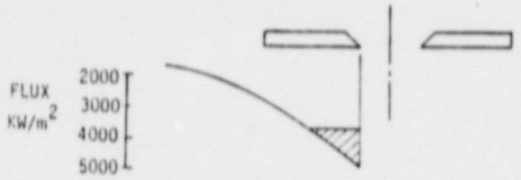

- WHITE SANDS TESTS
  KAOWOOL 3000 BOARD - 800 KW/M^2
  ZIRCONIA BOARD > 3000 KW/M^2

5.2.2 Aperture Face Insulation

The above chart indicates that during normal operation the aperture edge will be exposed to an incident solar flux of approximately 600 kW/m^2 (local maximum dependingon slope and tracking errors). In the event the concentrator stops tracking the sun, the focal point will move across the face of the aperture shield. The maximum local incident flux for this condition is not known at this time, but it is probably in excess of 4,000 kW/m^2.

BEC has conducted tests on Kaowool 3000 board and found no detectable damage upon long term (8 hour) exposure to solar flux of 800 kW/m^2. In addition, Zirconia board has been tested up to the limits of the White Sands Solar Test facility (3000 kW/m^2). These tests showed that hairline cracks appear after several hours of continuous exposure. The maximum rated use temperatures for these materials are 2500^{o}F and 3500^{o}F, respectively.

On this basis, a laminate aperture shield concept was selected: 1/2 inch zirconia board, 1 inch of Kaowool 3000 board, mounted to an Inconel 601 support ring.

This concept will provide adequate protection for normal operatior and mid-day sun acquisition. It is not known whether it is adequate for sustained loss of tracking, so a slew rate adjustment may be required to limit the exposure time.

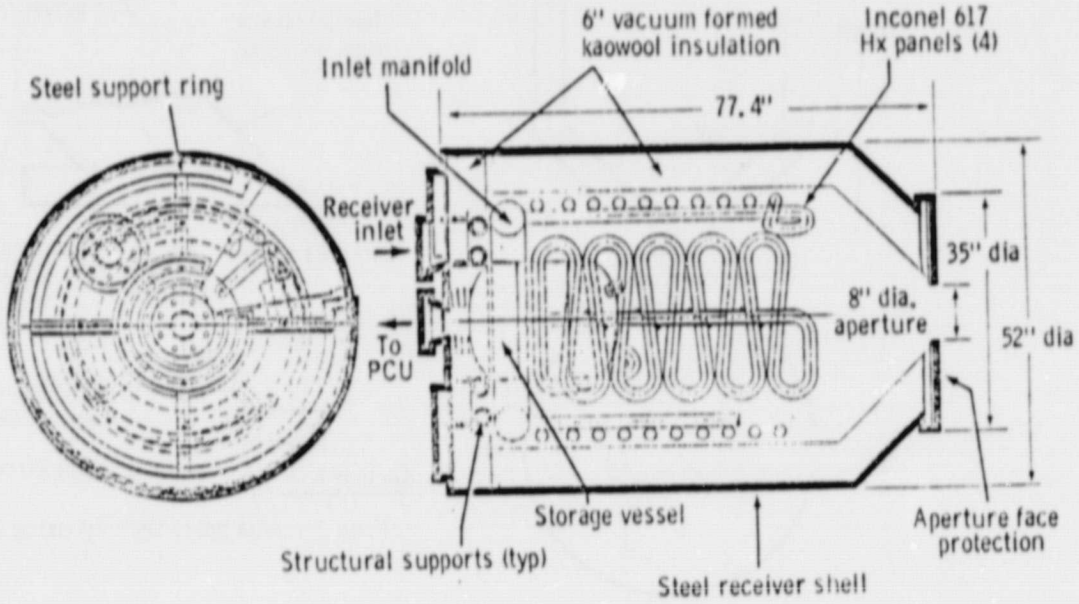

5.3 DESIGN FEATURES

5.3.1 Assembly Drawing

The drawing shows a top view and a sectional view of the ABSR. Each of the individual components are identified and discussed on the following pages.

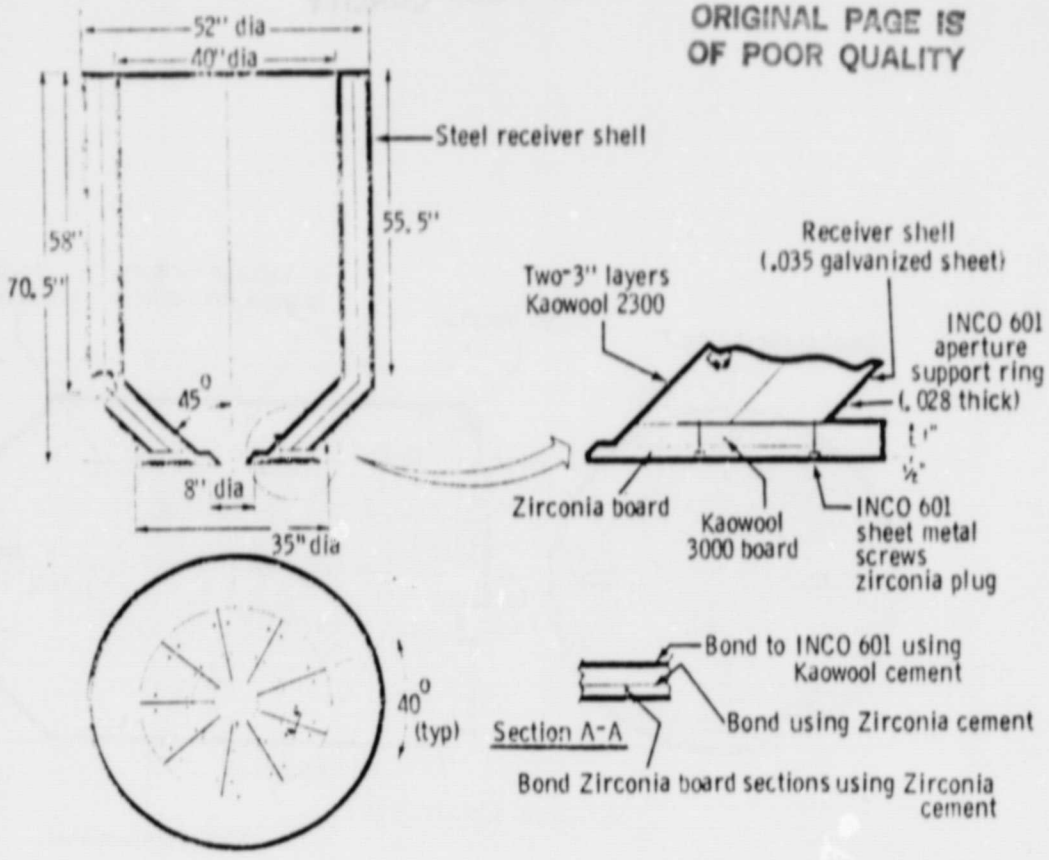

5.3.2 Structure and Insulation Details

The drawings show dimensions and details of the receiver wall structure and insulation. The receiver insulation is 12 PCF vacuum formed Kaowool. This is a rigid insulation, dimensionally stable, and capable of withstanding 2000°F continuously. The vacuum forming process is ideally suited for mass production. The cylindrical and conical sections are formed as an integral piece. The insulation could be formed as a full 6 inch thick section; however, it is more economical to make two 3 inch thick sections which nest together.

The .035 inch galvanized steel receiver shell was selected for adequate strength and durability.

The aperture rim shield uses materials and techniques developed and proven in the EPRI Bench Model Program, but modified for adaptability to mass production.

The receiver shell, insulation, and aperture shield form an integral unit which can be removed from the upper bulkhead to expose the heat exchanger - storage system discussed on the next page.

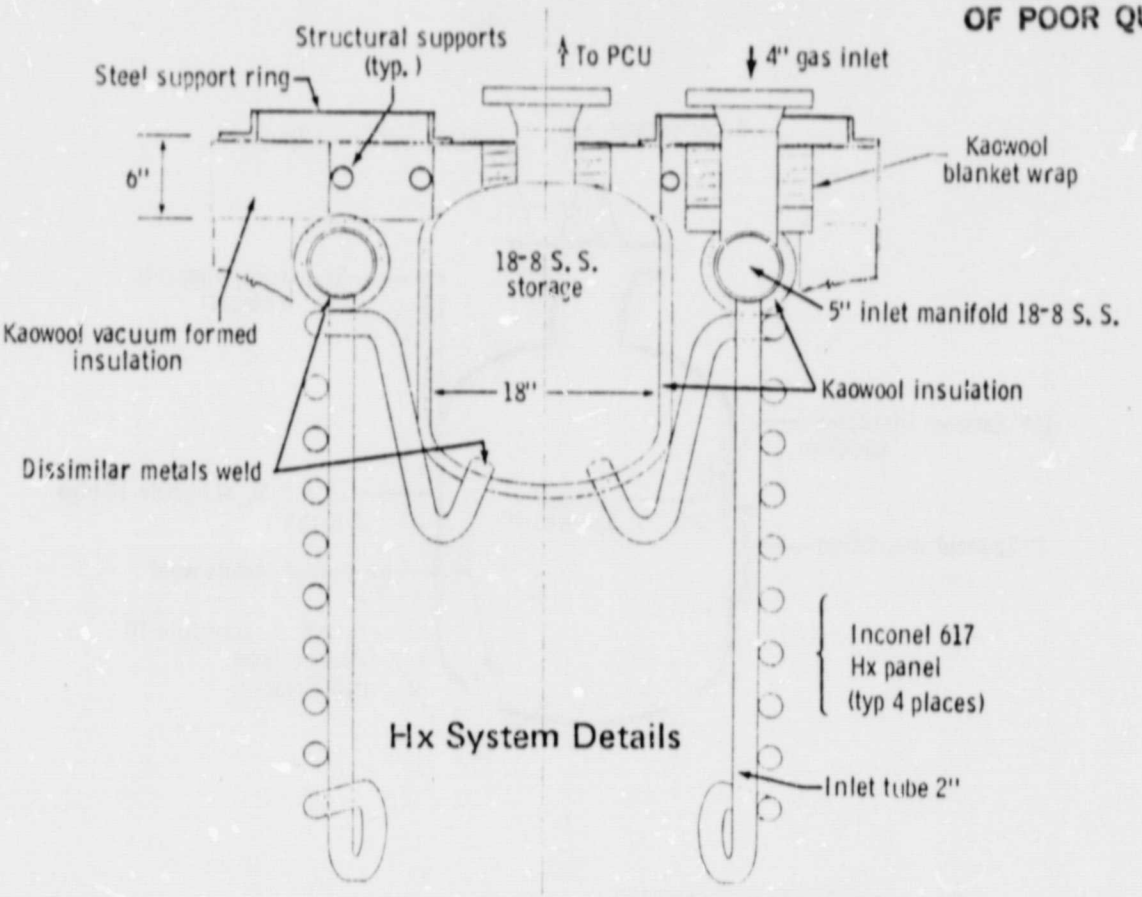

5.3.3 Heat Exchanger System Details

This drawing shows the heat exchanger and storage system mounted to the top steel support ring by hangers that allow movement in the radial direction to compensate for the thermal expansion of the inlet manifold and the storage tank. The hangers are welded to the manifold and storage tank (4 each). The upper end is threaded for attachment to the steel support ring.

Not identified in the drawing is the upper bulkhead which is a .035 inch galvanized steel lid situated between the steel support ring and the vacuum formed insulation block. The insulation block has two 8 inch diameter cut-outs to allow slipping the block over the manifold during assembly. The cutouts are subsequently filled with Kaowool blanket which is protected and retained with two-piece asbestos/steel ring grommets. The storage tank and inlet manifold are insulated with 1 inch of Kaowool to shield the stainless steel from the cavity environment.

The serpentine loops of the heat exchanger are supported by the inlet tube which is welded to the inlet manifold.

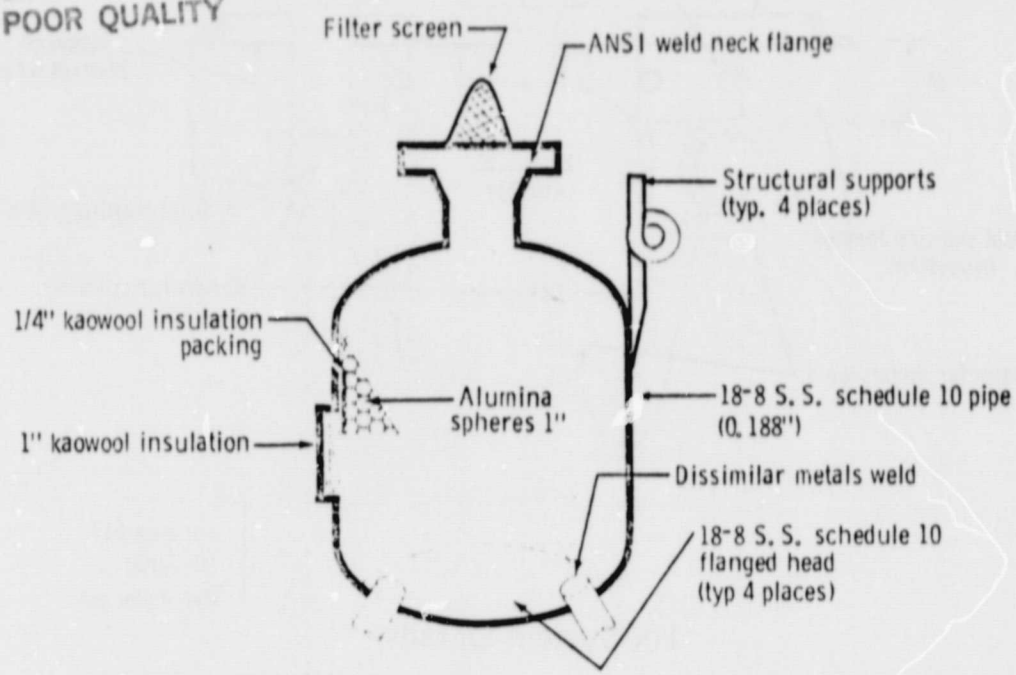

5.3.4 Storage System Details

The storage tank assembly is shown in the above drawing. The tank is welded from commercial schedule 10 stainless steel pipe and domes. The pebble bed is supported inside the tank by identical dome sections which have been perforated to 50 percent porosity with 3/16 inch holes to allow free flow of air. The support dome sections are trimmed to allow welding to the inside of the tank domes. The support domes prevent bed movement in any orientation.

The inner wall of the storage tank is lined with 1/4 inch of compressible packing to prevent the air stream from following a preferential path along the sides of the tank rather than passing through the bed. Differential thermal expansion will not present a problem since the alumina expands slightly less than the steel shell.

The drawing shows a screen filter located at the outlet flange. This commercial item can be installed for protection of the PCU, if required.